Site M0064[1]

T. Andrén, B.B. Jørgensen, C. Cotterill, S. Green, E. Andrén, J. Ash, T. Bauersachs, B. Cragg, A.-S. Fanget, A. Fehr, W. Granoszewski, J. Groeneveld, D. Hardisty, E. Herrero-Bervera, O. Hyttinen, J.B. Jensen, S. Johnson, M. Kenzler, A. Kotilainen, U. Kotthoff, I.P.G. Marshall, E. Martin, S. Obrochta, S. Passchier, N. Quintana Krupinski, N. Riedinger, C. Slomp, I. Snowball, A. Stepanova, S. Strano, A. Torti, J. Warnock, N. Xiao, and R. Zhang[2]

Chapter contents

[1] Andrén, T., Jørgensen, B.B., Cotterill, C., Green, S., Andrén, E., Ash, J., Bauersachs, T., Cragg, B., Fanget, A.-S., Fehr, A., Granoszewski, W., Groeneveld, J., Hardisty, D., Herrero-Bervera, E., Hyttinen, O., Jensen, J.B., Johnson, S., Kenzler, M., Kotilainen, A., Kotthoff, U., Marshall, I.P.G., Martin, E., Obrochta, S., Passchier, S., Quintana Krupinski, N., Riedinger, N., Slomp, C., Snowball, I., Stepanova, A., Strano, S., Torti, A., Warnock, J., Xiao, N., and Zhang, R., 2015. Site M0064. *In* Andrén, T., Jørgensen, B.B., Cotterill, C., Green, S., and the Expedition 347 Scientists, *Proc. IODP,* 347: College Station, TX (Integrated Ocean Drilling Program). doi:10.2204/iodp.proc.347.108.2015
[2] **Expedition 347 Scientists' addresses.**

Introduction

During Integrated Ocean Drilling Program (IODP) Expedition 347, cores were recovered from four holes at Site M0064 (Hanö Bay), with an average site recovery of 79%. The water depth was 60.5 m in Hole M0064A and 59.8 m in the other three holes, with a tidal range of <10 cm. Existing data sets, including seismic reflection profiles, were evaluated prior to each site to attempt to guide the initial drilling with an anticipated lithologic breakdown. The total time spent on station was 2.89 days.

Operations

Transit to Hole M0064A

The *Greatship Manisha* commenced transit to Site M0064 (proposed Site BSB-5) in Hanö Bay at 1215 h on 19 October 2013 and arrived on station by 1200 h on 20 October.

Hole M0064A

Operations in Hole M0064A commenced at 1200 h on 20 October 2013 with a remotely operated vehicle survey conducted to assess the seabed for the presence of WWII munitions. The survey covered Holes M0064A, M0064B, and M0064C. No evidence of any dangerous materials on the seabed was identified.

Following the survey, the vessel moved back to Hole M0064A and coring operations commenced (Table **T1**). The first four runs used the piston corer system (PCS) to recover clay. For Run 5, the nonrotating core barrel (NRCB) was used because of the presence of stiffer material indicative of the top of the diamicton unit. Run 6 used the push coring assembly (PCA) in an attempt to improve recovery. Following this, Runs 7–24 (16.05–34.5 meters below seafloor [mbsf]) used the NRCB, and Guar replaced seawater for pumping because of the increased sand content of the sediments. Run 25 was a PCA core, after a perceived failure to latch with the NRCB (no core recovered). Following the PCA, the string was flushed. The NRCB was lowered on the overshot, and latching was achieved. Coring with the NRCB continued for Runs 26–30. Runs 29 and 30 had no recovery, so a hammer sample (Run 31) was taken to prove the ground. The hammer sample recovered 0.08 m of gravel. The final NRCB (Run 32) core recovered 0.15 m of gravel with chalk beneath.

doi:10.2204/iodp.proc.347.108.2015

A total of 32 cores were recovered from Hole M0064A to 41.5 mbsf. Recovery for the hole was 66.82%.

Downhole logging operations started on 21 October at 1300 with drill pipe tripped to 1.5 m. The first tool string with the total gamma ray and induction tools reached only 5 mbsf. At 1515 h, the option of reaming the pipe to total depth, doing a wiper trip, and setting the pipe to 10.5 m was discussed, but as the ship required a heading change, the decision was made to abandon the downhole logging attempt at this hole. Logging operations were completed at 1520 h.

Hole M0064B

Following completion of operations in Hole M0064A, the vessel moved to Hole M0064B under dynamic positioning, and operations commenced at 1605 h on 21 October 2013. The second PCS run (3.3–6.6 mbsf) unexpectedly recovered coarse-grained sand. A third PCS run was attempted, with poor recovery. It was therefore decided to open hole in order to try and penetrate the sand feature. A final hammer sample taken at 10.1 mbsf confirmed that sand was still present at this depth, and because of potential damage to drilling equipment and the unanticipated lithology, the hole was terminated here.

A total of four cores were recovered from Hole M0064B to a maximum depth of 10.20 mbsf, with one open-hole section. Recovery for the hole was 96.94% when the open-hole section was discounted.

Hole M0064C

The vessel arrived over Hole M0064C at 1915 h on 21 October 2013, and drilling operations commenced. The first PCS core was recovered to deck at 1925 h. Three more PCS cores were recovered to deck before the top of the diamicton unit necessitated use of the NRCB.

Coring in Hole M0064C continued on 22 October, with 21 cores recovered by midday. This included one small interval of open holing to clean the hole and penetrate a possible obstruction that had resulted in zero recovery from the previous core run. Following a significant drop in recovery rates at 38.2 mbsf, a hammer sample was conducted to ascertain the exact lithology. Following this, five more NRCB cores were taken, with very limited recovery of rounded pebbles and gravel. A final hammer sample returned granite and chalk basement. The hole was terminated at target depth. Preparations were made for downhole logging. However, despite the hole being flushed and wiper trips being carried out to condition the hole, the hole collapsed from 9 mbsf. It was therefore not possible to conduct any logging operations.

A total of 35 core attempts were made in Hole M0064C, with one open-hole section of 2 m. The hole reached 45.10 mbsf, and hole recovery was 74.98% when the open-hole section was discounted.

Hole M0064D

Operations in Hole M0064D began at 1555 h on 22 October 2013. Based on the lithologies observed in the other holes at this site, it was decided that this hole should be cored at a new location, midway between Holes M0064A and M0064C, in an attempt to avoid the sand unit encountered in Hole M0064B and prevent the need for a second camera survey (as this hole lay on the A–C transect surveyed initially).

Operations began successfully in Hole M0064D with five piston cores being recovered. During recovery of the fifth core, a spline came off the overshot, but this was successfully retrieved using a magnet. As a soft diamicton was recovered in this run, the decision was made to change to the NRCB and continue operations.

NRCB Runs 6–13 recovered material from the diamicton layer to 23.4 mbsf. Run 14 was an open-hole run, using the insert bit to clear a blockage. Following this run, NRCB coring resumed to 33.90 mbsf. At this point, it was no longer possible to core, so an open-hole section was drilled, ending at 41.0 mbsf where a hammer sample was taken to prove the ground. The hammer sample recovered 0.2 m of gravel.

This marked the end of the hole (at 0755 h on 23 October), and the drill floor was prepared for downhole logging operations.

Downhole logging operations started in Hole M0064D on 23 October at 0715 h with rigging up the Weatherford logging setup while the drill pipe was tripped to 9 mbsf. The first tool string comprising the total gamma ray and induction tools reached 31 mbsf, and the second tool string comprising total gamma and spectral gamma ray tools reached 26 mbsf from where an uplog was started. Logging operations were finished at 1035 h.

A total of 21 cores were recovered from Hole M0064D. A further four recorded runs were open-hole sections with no recovery attempted. Hole recovery was 77.94% when open-hole sections were discounted.

Lithostratigraphy

At Site M0064, four holes were drilled: Hole M0064A to a total depth of 41.5 mbsf, Hole M0064B to 10.2

mbsf, Hole M0064C to 45.10 mbsf, and Hole M0064D to 41.2 mbsf. The top ~12 to ~15 m in each hole was retrieved by piston coring with nearly 100% recovery in Holes M0064A, M0064C, and M0064D. Hole M0062B terminated in a sand and gravel deposit (Fig. F1). Deeper than ~15 mbsf, the nonrotating core barrel was used to ~35 mbsf, with ~50% recovery in each hole, encountering different formation depths within each hole. A combination of nonrotating core barrel, push coring, open holing, and hammer sampling achieved advancement of the drill bit with nearly 100% recovery between ~35 and 38 mbsf in Holes M0064A and M0064C but with limited recovery deeper than this depth (see "Operations").

Lithostratigraphic divisions (Units I–IV; Fig. F2) are based on descriptions on the cut face of the split core and observations from smear slides (see "Core descriptions"). Units I and II are absent in Holes M0064B and M0064C.

Unit I

Intervals: 347-M0064A-1H-1, 0 cm, to 1H-1, 33 cm; 347-M0064D-1H-1, 0 cm, to 1H-1, 134 cm

Depths: Hole M0064A = 0–0.33 mbsf; Hole M0064D = 0–1.34 mbsf

Unit I is very dark greenish gray diatom-bearing clay, 0.33 to 1.34 m thick, largely homogeneous, but with weak parallel planar laminations at the base of the unit (Fig. F3). Laminae are black in color, and a smear slide from the base of the unit reveals a relatively large amount of opaque, possibly iron sulfide, minerals.

This unit was likely deposited in a brackish marine or lake environment with low terrigenous sediment input. For the base of the unit, a stratified water column, low oxygen, and a lack of benthic life may have allowed for preservation of lamination. Accumulation of organic matter may have formed the precursor to the iron sulfide minerals.

Unit II

Intervals: 347-M0064A-1H-1, 33 cm, to 1H-1, 60 cm; 347-M0064D-1H-1, 134 cm, to 1H-2, 25 cm

Depths: Hole M0064A = 0.33–0.6 mbsf; Hole M0064D = 1.34–1.75 mbsf

Unit II is greenish gray to very dark greenish gray sandy silt, 0.27 to 0.41 m thick. The silt is stratified with a coarser, more sand-rich upper part (Fig. F3). No fossils were found in the unit.

The sediment probably represents deposition in a shallow, oxidized, proglacial lake environment with relatively high terrigenous sedimentation rates.

Unit III

Subunit IIIa

Intervals: 347-M0064A-1H-1, 60 cm, to 3H-1, 85 cm; 347-M0064B-1H-1, 0 cm, to 1H-3, 24 cm; 347-M0064C-1H-1, 0 cm, to 2H-2, 116 cm; 347-M0064D-1H-2, 25 cm, to 3H-2, 87 cm

Depths: Hole M0064A = 0.6–7.15 mbsf; Hole M0064B = 0–2.94 mbsf; Hole M0064C = 0–5.96 mbsf; Hole M0064D = 1.75–7.87 mbsf

Subunit IIIb

Intervals: 347-M0064A-3H-1, 85 cm, to 3H-2, 73 cm; 347-M0064B-1H-3, 24 cm, to 2H-1, 130 cm; 347-M0064C-2H-2, 116 cm, to 3H-1, 69 cm; 347-M0064D-3H-2, 87 cm, to 4H-1, 50 cm

Depths: Hole M0064A = 7.15–8.53 mbsf; Hole M0064B = 2.94–4.6 mbsf; Hole M0064C = 5.96–7.29 mbsf; Hole M0064D = 7.87–9.3 mbsf

Unit III is dark grayish brown laminated clay and silty clay with dispersed clasts. The clay is rhythmically laminated by color on a centimeter scale and locally contains dispersed gravel clasts, sand, and sedimentary intraclasts. Inclined laminae and synsedimentary microfaults are also observed. Lamination is planar, parallel, and inclined, and in Subunit IIIb, it comprises distinct varve-like fining-upward silty clay to clay couplets. Subunit IIIa is more brown in color, whereas Subunit IIIb is more gray with an increase in silt toward the bottom of the unit. The bottom 3 cm of Subunit IIIa is dark brown and forms the boundary between Subunits IIIa and IIIb (Fig. F3). The contact between Subunits IIIa and IIIb is distinct in color, but there is no change in sediment texture and the lamination has a consistent orientation across the subunit boundary.

Deposition in a glacial lake is inferred for this unit. The inclined laminae, synsedimentary microfaults, and sedimentary intraclasts may indicate minor slumping due to an unstable sloping environment or high sedimentation rates. Outsized gravel clasts probably represent ice rafting.

Unit IV

Subunit IVa

Intervals: 347-M0064A-3H-2, 73 cm, to 18N-1, 0 cm; 347-M0064B-2H-1, 130 cm, to 5S-1, 10 cm; 347-M0064C-3H-1, 69 cm, to 17N-1, 0 cm; 347-M0064D-4H-1, 50 cm, to 15N-1, 0 cm

Depths: Hole M0064A = 8.53–26.5 mbsf; Hole M0064B = 4.6–10.2 mbsf; Hole M0064C = 7.29–25.7 mbsf; Hole M0064D = 9.3–25.4 mbsf

Subunit IVb

Intervals: 347-M0064A-18N-1, 0 cm, to 26N-1, 85 cm; 347-M0064C-17N-1, 0 cm, to 28N-1, 0 cm; 347-M0064D-15N-1, 0 cm, to end of hole

Depths: Hole M0064A = 26.5–36.35 mbsf; Hole M0064C = 25.7–36.7 mbsf; Hole M0064D = 25.4–41.20 mbsf

Subunit IVc

Intervals: 347-M0064A-26N-1, 85 cm, to end of hole; 347-M0064C-28N-1, 0 cm, to end of hole

Depths: Hole M0064A = 36.35–41.5 mbsf; Hole M0064C = 36.7–45.0 mbsf

Unit IV is composed of moderately to poorly sorted coarse-grained sediments with variable gravel abundances and sand content in the matrix. Subunit IVa consists primarily of clast-rich stratified muddy diamicton and sandy gravel. Within the diamicton, contorted mud stringers and laminae, as well dark color banding, are observed (Fig. F3). Subunit IVb is dominated by massive, clast-poor, sandy diamicton (Fig. F3). Occasional potential clast alignment fabrics were observed in this facies. Subunit IVc consists of stratified sandy clayey silt with dispersed clasts and thin intervals of diamicton. In this latter subunit, a large variation in clast abundances is observed over relatively short depth intervals.

Unit IV was deposited in an ice-influenced depositional environment. Subunit IVa shows evidence of meltwater flow and minor gravity flow, as well as features of an ice-contact outwash plain. Subunit IVb probably represents an ice-proximal deposit with massive diamicton originating from either subglacial processes, glacigenic debris flow, or glaciomarine/glaciolacustrine deposition. Subunit IVc likely originated in an ice-influenced aquatic depositional environment, with variations in clast abundances due to changes in glaciomarine or glaciolacustrine deposition.

Biostratigraphy

Diatoms

Qualitative analysis of diatom community composition was carried out on one sample from Site M0064 (Table T2). Sample 347-M0064A-1H-1, 0 cm, contains a typical Baltic Sea assemblage (Andrén et al., 2000; Snoeijs et al., 1993–1998). This assemblage contains both diatoms and chrysophycean cysts. All other samples from Hole M0064A and all samples from Holes M0064B and M0064C, including core tops, were barren of siliceous microfossils. Reworked Cretaceous foraminifers and coccolithophorids were found in Section 347-M0064C-3H-2, 0 cm.

Foraminifers and ostracods

A total of 29 samples (21 taken offshore from core catchers and 8 from regular sections during the Onshore Science party [OSP]) from Site M0064 were prepared for foraminiferal and ostracod analysis. Foraminifers do not occur in the sediments sampled at this site. The lack of foraminifers suggests that low oxygen and/or salinity may have prevented the occurrence of foraminifers in the basin. Almost no microfossils >63 µm were present, even in the upper dark brown sediment (Unit I, Core 1, Section 1 in each hole), potentially suggesting low-oxygen conditions, a theory supported by the laminated nature of sediments in this interval (see **"Lithostratigraphy"**). However, a few testate amoebae occurred in Sample 347-M0064D-1H-1, 15–17 cm.

Only one juvenile ostracod valve of *Paracyprideis* sp. was found at this site at 0.16 mbsf in Hole M0064D; the sediments were otherwise barren with respect to ostracods.

Palynological results

Site M0064 is situated in the central part of the southern Baltic Sea. The vegetation of the borderlands in that region belongs to the cool temperate forest zone with mixed coniferous and deciduous trees. However, the boreal-forest vegetation zone is very close to the site. The palynological analyses for this site were carried out on Hole M0064A.

A total of 12 samples from Hole M0064A were analyzed (see PalyM0064.xls in PALYNOLOGY in "**Supplementary material**"). However, the palynomorphs in all samples appeared to have been degraded/oxygenated to a high degree, and no sample contained enough palynomorphs in situ to yield statistically relevant data. Only five samples contained in situ pollen preserved well enough to identify nonsaccate pollen. The pollen concentration per cubic centimeter varied from 0 to ~1000 grains, which is a factor 500 to 1000 lower than the concentration encountered in samples with good preservation at other sites.

Two samples from the depth interval of ~6.5–8.5 mbsf contain a few *Pinus* (pine), *Picea* (spruce), *Betula* (birch), *Juniperus* (juniper), and *Quercus* (oak) pollen grains. The sample at ~6.5 mbsf furthermore contains several steppe element pollen grains (*Artemisia*/Chenopodiacea). This assemblage may imply a late glacial/early Holocene age, but as stated above, the statistical relevance of the data is too low for a reliable age estimate.

Samples deeper than ~15 mbsf contain high amounts of degraded material, and there were often more reworked than in situ pollen. In Sample 347-

M0064A-12H-CC, the number of reworked dinoflagellate cysts surpassed that of reworked pollen grains. Some of these cysts could be identified to the genus level and thus allowed age estimation for the reworked material. The genera comprise *Apectodinium*, *Wetzeliella*, and *Charlesdowniea* (Fig. F4). The reworked material thus is of Paleogene origin (Powell, 1992; K. Dybkjær, pers. comm., 2014). Reworked pollen includes *Picea* and *Pinus* as well as *Carya* pollen grains.

Geochemistry

Interstitial water

Pore water samples from Site M0064 were recovered from the upper 16 m of the cored interval. For Holes M0064A, M0064C, and M0064D, this interval is composed of diamicton overlain by 7–9 m of glacial lake clays (see "Lithostratigraphy" and "Biostratigraphy"). For Hole M0063B, the lake clays transition into a sand layer at 4.6 mbsf. Low organic matter concentrations in these sediments and the present-day brackish conditions at the site govern the pore water profiles.

Salinity variations: chloride, salinity, and alkalinity

Pore water chloride (Cl^-) and salinity profiles (Fig. F5A–F5B; Tables T3, T4) illustrate good agreement between holes and between salinity measurements made shipboard with a refractometer and derived from Cl^- (Cl^- based salinity; Fig. F5C). Salinity is 13–14 in the shallowest sample at 1.35 mbsf, increases to ~15 at 6–8 mbsf, and then drops again to 11–12 toward the bottom of the holes. Alkalinity values are very low at Site M0064 (2–5 meq/L), with minor differences between holes; in Holes M0064A and M0064D, alkalinity decreases from ~6 meq/L at the surface to 3 meq/L at depth, whereas in Holes M0064B and M0064C alkalinity is relatively constant between 3 and 4 meq/L (Fig. F5D).

Organic matter degradation: sulfate, ammonium, phosphate, iron, manganese, pH, bromide, and boron

No methane or hydrogen sulfide measurements were conducted at this site. Pore waters record evidence of only minor organic matter degradation likely due to the overall low concentrations of organic matter in the sediments (see below). Sulfate (SO_4^{2-}) decreases from 10 mM in the shallowest samples to 5 mM at depth (Fig. F6A). A plot of SO_4/Cl (Fig. F6B) suggests that the SO_4^{2-} depletion represents sulfate reduction rather than dilution by low-salinity pore waters.

Pore water ammonium (NH_4^+; Fig. F6C) indicates minor release from organic matter degradation, with values of 0.1–0.3 mM in the shallowest samples increasing to 0.4 mM at depth (Table T3). Pore water phosphate (PO_4^{3-}) concentrations are low (~0.01 mM) throughout most of the sampled interval, with a peak of 0.05 mM in the uppermost 3 mbsf (Fig. F6D). Both dissolved iron (Fe^{2+}) and manganese (Mn^{2+}) concentrations are scattered with broad peaks at 5–10 mbsf (Fig. F6E–F6F). Dissolved Fe^{2+} concentrations peak at ~200 µM, whereas in Hole M0064D the deepest sample returns to a higher value of 230 µM. Dissolved Mn^{2+} concentrations peak at 60–70 µM, with values of 20–30 µM in the shallowest samples and 10–25 µM in the deepest samples. pH has a slight and broad minimum of ~7.5 at 5–10 mbsf, with values of ~7.7 at the top and bottom of the sampled interval (Fig. F6G).

Pore water bromide (Br^-) concentrations (Fig. F7A) vary over a narrow range of 0.27–0.35 mM and follow the pattern observed for salinity and Cl^- such that the Br/Cl ratio is almost constant with depth (Fig. F7B), reflecting the seawater ratio. All holes have a similar pattern for boron (B), with surface concentrations of 150–190 µM that decrease to ~60 µM by 6 mbsf and maintain similar concentrations deeper than that depth (Fig. F7C). The shallowest B/Cl ratios are similar to the seawater ratio (Fig. F7D), but underlying ratios indicate uptake of B, possibly by weathering reactions or ion exchange.

Mineral reactions

Sodium, potassium, magnesium, and calcium

Concentrations of Na^+ are relatively constant with depth and between holes, with a range of 130–240 mM (Fig. F8A; Table T3). Unlike other sites, K^+ profiles at Site M0064 do not follow the same pattern as Na^+. Instead, the K^+ profile is similar to boron, with the highest concentrations of ~4 mM in the shallowest sample and values that decrease to 1.5–2 mM before leveling off deeper than ~6 mbsf (Fig. F8B). Pore water Mg^{2+} profiles are similar to Na^+, with a narrow range of concentrations spanning 16–23 mM with depth (Fig. F8C). Pore water Ca^{2+} concentrations increase gradually from ~10 mM in the shallowest samples to a broad peak of ~25 mM between 6 and 10 mbsf, depending on the hole (Fig. F8D). Element to Cl^- ratios for the major cation concentrations highlight differences from seawater ratios (Fig. F8E–F8H). Both Na/Cl and Mg/Cl exhibit little variation from

seawater values. Like B/Cl, the K/Cl ratios decrease to values below the seawater ratio, again suggesting weathering reactions or ion exchange as a sink. All Ca/Cl ratios plot well above the seawater values, indicating a solid phase source of Ca^{2+} at depth.

Strontium, barium, lithium, and silica

Strontium (Sr^{2+}) concentrations are similar to Ca^{2+} profiles, with a gradual increase from 40 to 55 µM in the shallowest samples and a broad peak of ~125 µM at 8–10 mbsf (Fig. F9A). Concentration profiles of lithium (Li^{+}) are similar to both Ca^{2+} and Sr^{2+}. Li concentrations increase gradually from ~10 µM in the uppermost sample to a broad peak of ~15 µM at 8–10 mbsf (Fig. F9B). Dissolved silica (H_4SiO_4) concentrations increase subtly from ~200 µM in the shallowest sample to ~325 µM at 10 mbsf (Fig. F9C). Pore water barium (Ba^{2+}) concentrations are very low at Site M0064, with values of 0.1–0.3 µM (Fig. F9D).

Sediment

Carbon content

The total carbon (TC) content at Site M0064 varies from 0.3 to 3.5 wt% across holes (Table T5; Fig. F10A). The highest total organic carbon (TOC) values (~2.3 wt%) occur in the uppermost ~0.70 m of the investigated profile, suggesting higher organic matter input during the more recent deposition of brackish-marine sediments, whereas the underlying freshwater and glaciolacustrine deposits are characterized by low TOC values of <0.4 wt% (Table T5; Fig. F10B).

The total inorganic carbon (TIC) content at Site M0064 increases with depth in the upper ~12 mbsf, reaching values of ~3.2 wt% (Table T5; Fig. F10C). The TIC content stays slightly elevated in the diamicton (lithostratigraphic Subunit IVa) and drops to an average value of 1.8 wt% deeper than ~20 mbsf.

Sulfur content

The total sulfur (TS) content is generally <0.5 wt% in sediments from the Hanö Bay (Table T5; Fig. F10D), with high values of 0.8–1.5 wt% being present only in the uppermost sediments (<1 mbsf). It is interesting to note that the lowest values of TS occur in the upper 1–7 mbsf (lithostratigraphic Subunit IIIa), where TOC values are slightly higher compared to the deeper sediment intervals.

Physical properties

This section summarizes the preliminary physical results from Site M0064. Four holes were drilled at this site. Hole M0064A was drilled to 41.5 mbsf, Hole M0064B was drilled to 10.2 mbsf, Hole M0064C was drilled to 45.10 mbsf, and Hole M0064D was drilled to 41.2 mbsf. We focus on Hole M0064A because it is the only hole in which all of the lithostratigraphic units described at Site M0064 were recovered (see "Lithostratigraphy"). Although all physical property measurements described in "Physical properties" in the Methods chapter (Andrén et al., 2015) were conducted at Site M0064, discrete thermal conductivity data are too sparsely distributed to exhibit any discernable downcore trend and noncontact electrical resistivity data show little variability.

Natural gamma radiation

High-resolution natural gamma ray (NGR) exhibits relatively little variability in Hole M0064A (Fig. F11). NGR values are low within lithostratigraphic Unit I (~7 cps) and increase rapidly toward the base of lithostratigraphic Unit II, which could reflect lower water content in this unit (see "Lithostratigraphy"). NGR values decrease at the lithostratigraphic Unit II/Subunit IIIa boundary and are relatively constant (~11 cps) in lithostratigraphic Subunit IIIa. NGR exhibits an increasing trend within lithostratigraphic Subunit IIIb. The negative excursions that occur throughout lithostratigraphic Unit III (including Subunits IIIa and IIIb) may correspond to beds of silty sand (see "Lithostratigraphy"). NGR values increase abruptly at the Subunit IIIb/IVa boundary to the maximum values (~17 cps) observed in Hole M0064A. Lithostratigraphic Unit IV is characterized by relatively constant NGR values of ~10 cps, except for lithostratigraphic Subunit IVb, which exhibits several intervals of reduced NGR (~5–10 cps).

Shipboard magnetic susceptibility

Magnetic susceptibility increases through lithostratigraphic Units I and II and is relatively constant in lithostratigraphic Subunit IIIa (Fig. F11). Lithostratigraphic Subunit IIIb is characterized by a slight increasing trend. Magnetic susceptibility increases sharply at the lithostratigraphic Subunit IIIb/IVa boundary, reflecting a lithologic change from clay and silty clay to diamicton (see "Lithostratigraphy"). Magnetic susceptibility is relatively constant in lithostratigraphic Unit IV, except for a large excursion visible at ~13 mbsf (Subunit IVa) and another increase that occurs at the Subunit IVa/IVb boundary.

Color reflectance

Lithostratigraphic Units I, II, and III are distinguished by differing color reflectance trends that are most apparent in the b* parameter (Fig. F11). In

Units I and II, b* exhibits a decreasing trend (more blue) from the top of the hole to ~1.3 mbsf, where values abruptly increase at the Unit II/Subunit IIIa boundary. Values for b* are relatively high (more yellow) in the upper interval of lithostratigraphic Subunit IIIa and then decrease at ~5 mbsf and increase again at ~6–6.6 mbsf to the highest values observed in Hole M0064A. At the Subunit IIIa/IIIb boundary, b* values decrease abruptly. In Subunit IIIb and the uppermost interval of Subunit IVa, b* values exhibit a decreasing trend. From ~16 mbsf to the bottom of the hole, b* exhibits a modal value of ~5.

Density and *P*-wave velocity

Dry density is generally low (<1 g/cm^3) in Units I and II and Subunit IIIa, with a positive excursion near the Subunit IIIa/IIIb boundary (Fig. **F11**). Values in Subunit IIIb increase to ~2 g/cm^3. At the Subunit IIIb/IVa boundary, dry density decreases again (<1 g/cm^3) and then increases in the lower interval of Subunit IVa (to ~2 g/cm^3). Dry density remains relatively constant through the bottom part of Hole M0064A.

Gamma density and *P*-wave velocity were both measured at 2 cm intervals during the offshore phase of Expedition 347 (Fig. **F12**). Gamma density values measured on the multisensor core logger (MSCL) are moderately well correlated with the discrete bulk density measurements performed during the OSP (r^2 = 0.5; Fig. **F12**). The shipboard *P*-wave velocity is not well correlated with the discrete *P*-wave measurements performed during the OSP (r^2 = 0.34; Fig. **F12**).

Paleomagnetism

Magnetic susceptibility measurements and simplified analyses of the natural remanent magnetization (NRM) were made on discrete specimens of known volume and mass (see **"Paleomagnetism"** in the "Methods" chapter [Andrén et al., 2015]). A total of 41 discrete samples were taken from Holes M0064A (16 samples), M0064C (14 samples), and M0064D (11 samples) at intervals of ~25 and 50 cm. The magnetic properties of this relatively small sample population varied. Magnetic susceptibility (χ) is relatively uniform between 8 and 2 mbsf, comprising Subunits IIIb (top) and IIIa and Units II and I. From ~8 to ~12 mbsf, χ ranges between ~0.024 × 10^{-6} m^3/kg and 0.39 × 10^{-6} m^3/kg within Subunits IVa and IIIb. The intensity of the NRM also varied over several orders of magnitude, from a maximum of 59 A/m at ~9.5 mbsf in Subunit IIIb to 0.02 × 10^{-3} A/m in the top part of Subunit IVa. There was also considerable variation in the lower part of Subunit IVa, the top part of Subunit IVa, and Subunits IIIa and IIIb, with enhanced NRM intensities associated with laminated clay, silt clays, and dark greenish gray sandy silt subunits.

Paleomagnetic pilot samples were grouped into two categories according to their response to alternating field (AF) demagnetization. Category 1, containing samples from Subunit IVa (clast-rich stratified muddy diamicton and sandy gravel), has unstable magnetizations. Category 2, associated with Subunit IIIa, has a stable magnetic remanence but inclinations that differ between Hole M0064A (shallow) and Hole M0064C (steep).

Discrete sample measurements

A total of 41 discrete paleomagnetic samples were obtained from Holes M0064A, M0064C, and M0064D at 25 and 50 cm intervals.

Magnetic susceptibility

The results of the magnetic analyses are shown in Figure **F13.** Magnetic susceptibility (χ) ranges between ~0.024 × 10^{-6} m^3/kg and 0.39 × 10^{-6} m^3/kg, and a general declining trend in χ is evident from Unit II to the top of Subunit IVa, which appears to be positively related to a decrease in sample wet density. The intensity of the NRM, however, displays a wide range over 3 orders of magnitude, suggesting variable magnetic mineralogy and/or efficiency of recording of the geomagnetic field. Only one sample was recovered from Subunit IVb (massive clast-poor sandy diamicton), and it has an intermediate χ value close to 0.2 × 10^{-6} m^3/kg. The top of Subunit IVa has the lowest χ values of the entire core sampled. There are several samples in the top of Subunits IVa and IIIb that have significantly higher χ than the background level for these units, which is between 0.01 × 10^{-6} and 0.2 × 10^{-6} m^3/kg, showing values between 0.3 × 10^{-6} and 0.8 × 10^{-6} m^3/kg.

Natural remanent magnetization and its stability

The NRM intensity spans 3 orders magnitude, between 0.02 × 10^{-3} A/m and 59 × 10^{-3} A/m. The NRM intensity displays a weak positive relationship with χ in Subunits IVa and IIIb; however, this relationship is disturbed by the occurrence of samples with relatively high NRM intensity compared to χ. Only two categories of response to AF demagnetization were observed in the pilot samples (Fig. **F14**). The pilot sample taken from Subunit IVb at ~27.03 meters composite depth (mcd) (Category 2), which contains a massive clast-poor sandy diamicton, displays a linear orthogonal vector that trends toward the origin during AF demagnetization, and the carrier(s) of remanence have medium to low coercivity with a re-

sidual NRM intensity of ~10% after the treatment at 40 mT. Category 2 has relatively high inclinations, between 70° and 80°. Category 1 samples do not contain a stable magnetic remanence.

Paleomagnetic directions

Core sections recovered from Holes M0064A, M0064C, and M0064D are characterized by scattered inclination data and between-hole differences, such as the systematic 45° difference between Hole M0064C and Hole M0064D between 10 and 5 mbsf. We conclude that the geomagnetic field has not been recorded sufficiently well at this site to allow the data to be used for relative paleomagnetic dating.

Stratigraphic correlation

Four holes were drilled at Site M0064: Holes M0064A (41.5 mbsf), M0064B (10.2 mbsf), M0064C (45.10 mbsf), and M0064D (41.20 mbsf). The meters composite depth scale for Site M0064 was based on correlation of magnetic susceptibility and natural gamma between holes (Fig. F15). At this site, the offset and overlap between adjacent holes was monitored (using data from every other core) by measuring Fast-track magnetic susceptibility (see "Physical properties") during the drilling process. These data proved to be an efficient tool to monitor and adjust the drilling process to maximize composite core recovery. Sediment cores were also logged with a standard MSCL to enable more precise hole-to-hole correlation and to construct a composite section for Site M0064 (Fig. F15). Before analysis, all magnetic susceptibility data were cleaned, removing any outliers from the measurements from the top of each section. The correlation was checked against scanned core slab images and lithologic descriptions. The depth offsets that define the composite section for Site M0064 are given in Table T6 (affine table).

Correlation between the magnetic susceptibility data in Holes M0064A, M0064B, M0064C, and M0064D is good, enabling the production of a continuous splice record for this site (Table T7). The accuracy of the correlation was visually checked from scanned core slab images using Corelyzer software. At Site M0064, correlation was straightforward to 11.54 mcd (Section 347-M0064C-3H-3, 41 cm). The lowermost part of Hole M0064C was appended in the splice record. No compression or expansion corrections were applied to the data, so the offset within each core was equal for all points. Thus, it is possible that some features are not similarly aligned between holes.

Seismic units

Seismic sequence boundary-sediment core-MSCL log (magnetic susceptibility) correlations are shown in Figure F16. Correlation is based on the integration of seismic data and lithostratigraphy (see "Lithostratigraphy"). Two-way traveltime values were calculated for each lithostratigraphic unit boundary using sound velocity values measured during the OSP (see "Physical properties"; Table T8). Lithostratigraphic unit boundaries were examined at these calculated two-way traveltime values to define the extent of agreement between seismic boundaries and actual lithologic and/or physical property disconformable surfaces. Uncertainties in the time-depth function and the effects of gas-saturated sediments could have resulted in inconsistencies between seismic features, sedimentological observations from cores, and MSCL logs.

Seismic Unit I

Two-way traveltime: 0.0829 ms
Lithology: very dark greenish gray diatom-bearing clay (lithostratigraphic Unit I)
Depths: 0–0.33 mbsf (M0064A), 0–1.34 mbsf (M0064D)

Unit I corresponds to a thin, relatively transparent unit in the uppermost part of the seismic profile.

Seismic Unit II

Two-way traveltime: 0.0835 ms
Lithology: greenish gray to very dark greenish gray sandy silt
Depths: 0.33–0.6 mbsf (M0064A), 1.34–1.75 mbsf (M0064D)

Unit II coincides with the uppermost strong reflector visible in the seismic profile. Magnetic susceptibility values are low in both Units I and II.

Seismic Unit III

Two-way traveltime: 0.0938 ms
Lithology: dark grayish brown laminated clay and silty clay with dispersed clasts (lithostratigraphic Subunits IIIa and IIIb)
Depths: 0.6–8.53 mbsf (M0064A), 0–4.6 mbsf (M0064B), 0–7.29 mbsf (M0064C), 1.75–9.3 mbsf (M0064D)

Seismic Unit III shows a slightly irregular internal structure and a strong reflector at its base. Magnetic susceptibility values are relatively low and comparatively stable throughout this unit. However, they in-

crease rapidly downcore at the lower boundary of Unit III.

Seismic Unit IV

Seismic Subunit IVa

Two-way traveltime: 0.1116 ms
Lithology: stratified muddy diamicton and sandy gravel (lithostratigraphic Subunit IVa)
Depths: 8.53–26.5 mbsf (M0064A), 4.6–10.2 mbsf (M0064B), 7.29–25.7 mbsf (M0064C), 9.3–25.4 mbsf (M0064D)

Subunit IVa correlates relatively well with strong irregular reflectors visible in the seismic profile. Magnetic susceptibility values increase rapidly at the upper boundary of Subunit IVa and remain, with some variability, relatively high. The seismic profile shows strong parallel structures in the lowermost part of this unit, suggesting a possible unconformity or erosional contact between Subunits IVa and IVb.

Seismic Subunit IVb

Two-way traveltime: 0.1241 ms
Lithology: primarily massive diamicton, possible shear fabrics (lithostratigraphic Subunit IVb)
Depths: 26.5–36.35 mbsf (M0064A), 25.7–36.7 mbsf (M0064C), 25.4–41.20 mbsf (M0064D)

Magnetic susceptibility values are slightly lower in Subunit IVb than in Subunit IVa. The seismic profile of Subunit IVb shows faint irregular structures that are slightly stronger and clearer than in the following subunit.

Seismic Subunit IVc

Two-way traveltime: 0.1332 ms
Lithology: stratified sandy clayey silt with dispersed clasts and diamicton (lithostratigraphic Subunit IVc)
Depths: 36.35–41.5 mbsf (M0064A), 36.7–45.0 mbsf (M0064C)

This unit is followed by sedimentary bedrock based on the seismic profile.

Downhole measurements

Logging operations

Hole M0064A was drilled to 41.5 m drilling depth below seafloor (DSF). In preparation for logging, the hole was circulated with seawater and the drill string was pulled back in the hole to 2 m wireline log depth below seafloor (WSF). Logging operations started in Hole M0064A with rigging up of the Weatherford logging setup.

Before the running in the hole of the first tool string could be started, a problem with the winch was noticed. After the problem was fixed, the gamma ray tool (MCG)/array induction tool (MAI) tool string, measuring total gamma ray and induction, could be run in the hole, and a downlog was started. The seafloor was picked up by the gamma ray, and the tool string came out of the pipe. Immediately, a sudden drop in tension indicated that the tool string set up at ~5 m WSF. Logging operations were abandoned in this hole after this unsuccessful attempt. During rig-up of the logging setup, the pipe was completely out of the hole, probably causing the top of the hole to collapse.

Downhole logging measurements in Hole M0064D were performed after completion of coring to a total depth of 41.2 m DSF. In preparation for logging, the hole was circulated with seawater and the pipe was pulled back to ~7.6 m WSF.

For downhole logging in Hole M0064D, two tool strings were deployed:

- MCG/MAI tool string, measuring natural gamma ray and electrical resistivity; and
- MCG/spectral gamma ray tool (SGS) tool string, measuring total gamma ray and spectral gamma ray.

The MCG/MAI tool string was lowered and downlogged to 31 m WSF. The hole was then uplogged to the seafloor. The wireline depth to the seafloor was determined from the step increase in gamma ray values.

After this, the MCG/SGS tool string was lowered and reached 26.4 m WSF while downlogging. The hole was then uplogged to the seafloor. The tools provided continuous and good quality log data.

Logging units

Hole M0064D is divided into three units on the basis of the logs (Fig. **F17**). The uplog was used as the reference to establish the wireline log depth below seafloor depth scale.

Logging Unit 1: base of drill pipe to14.7 m WSF

Natural gamma ray in this logging unit generally increases with depth, with some fluctuations around 10 and 13 m WSF. The negative excursions that occur in this logging unit may correspond to the beds of silty sand described in lithostratigraphic Unit III (see **"Lithostratigraphy"**). At 14.7 m WSF is a sudden drop in NGR values. Resistivity slightly increases from 9 to 13 m WSF and then decreases to its lowest value at 15 m WSF.

Logging Unit 2: 14.7–21 m WSF

After the drop in NGR at 15 m WSF, natural gamma ray remains constant in logging Unit 2, with a slight increase at the bottom of the unit. Thorium values are higher in logging Unit 2 than in logging Unit 1, with large fluctuations around 20 m WSF. Resistivity increases with depth in logging Unit 2 because of compaction.

Logging Unit 3: 21–31 m WSF

Deeper than 21 m WSF, the resistivity log shows constant values. The natural gamma ray log shows a slight decrease but a different trend for the different tool strings used. Total gamma ray measured with the MCG/MAI tool string is ~20 gAPI lower than the one measured with the MCG/SGS tool string. This may be due to changing borehole conditions.

References

Andrén, E., Andrén, T., and Kunzendorf, H., 2000. Holocene history of the Baltic Sea as a background for assessing records of human impact in the sediments of the Gotland Basin. *Holocene,* 10(6):687–702. **doi:10.1191/09596830094944**

Andrén, T., Jørgensen, B.B., Cotterill, C., Green, S., Andrén, E., Ash, J., Bauersachs, T., Cragg, B., Fanget, A.-S., Fehr, A., Granoszewski, W., Groeneveld, J., Hardisty, D., Herrero-Bervera, E., Hyttinen, O., Jensen, J.B., Johnson, S., Kenzler, M., Kotilainen, A., Kotthoff, U., Marshall, I.P.G., Martin, E., Obrochta, S., Passchier, S., Quintana Krupinski, N., Riedinger, N., Slomp, C., Snowball, I., Stepanova, A., Strano, S., Torti, A., Warnock, J., Xiao, N., and Zhang, R., 2015. Methods. *In* Andrén, T., Jørgensen, B.B., Cotterill, C., Green, S., and the Expedition 347 Scientists, *Proc. IODP,* 347: College Station, TX (Integrated Ocean Drilling Program). **doi:10.2204/iodp.proc.347.102.2015**

Powell, A.J. (Ed.), 1992. *A Stratigraphic Index of Dinoflagellate Cysts:* London (Springer).

Snoeijs, P., Vilbaste, S., Potapova, M., Kasperoviciene, J., and Balashova, J. (Eds.), 1993–1998. *Intercalibration and Distribution of Diatom Species in the Baltic Sea* (Vol. 1–5): Uppsala, Sweden (Opulus Press).

Publication: 20 February 2015
MS 347-108

Figure F1. Graphic lithology log summary, Holes M0064A–M0064D.

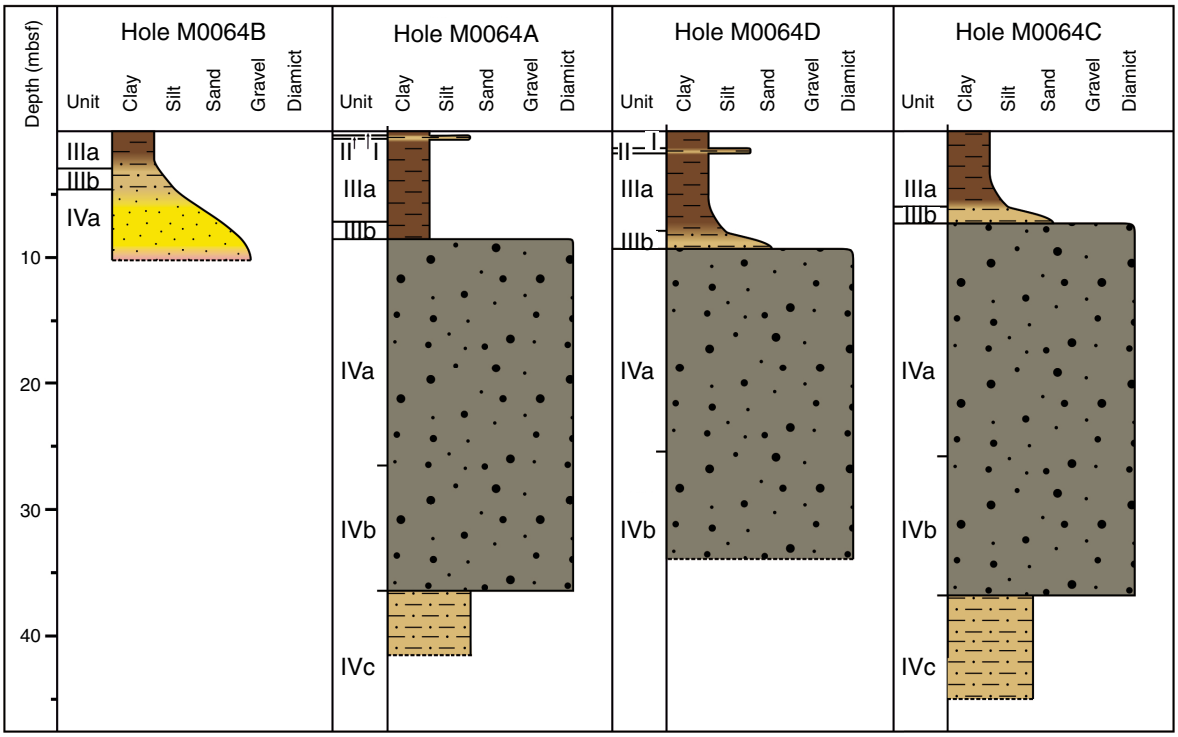

Figure F2. Graphic lithology log summary, Site M0064. Depths quoted represent boundary depths from Holes M0064D (Unit I to the base of Subunit IVa) and M0064C (from the top of Subunit IVb to the base of Subunit IVc).

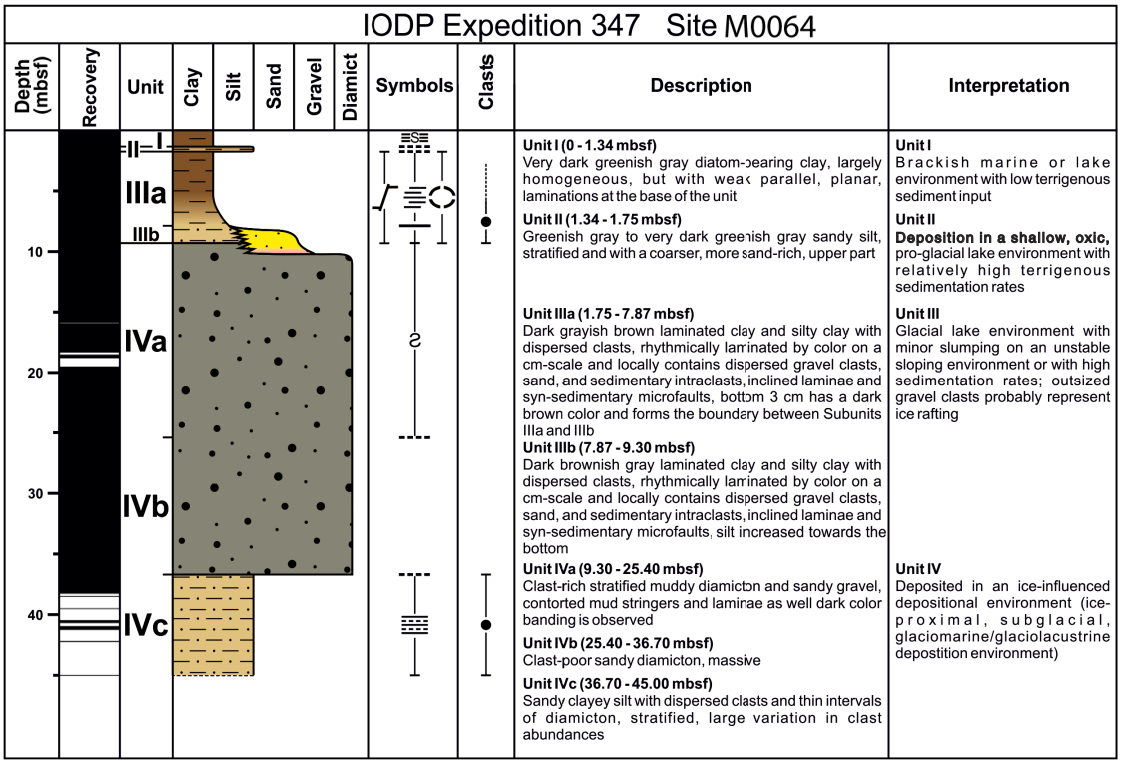

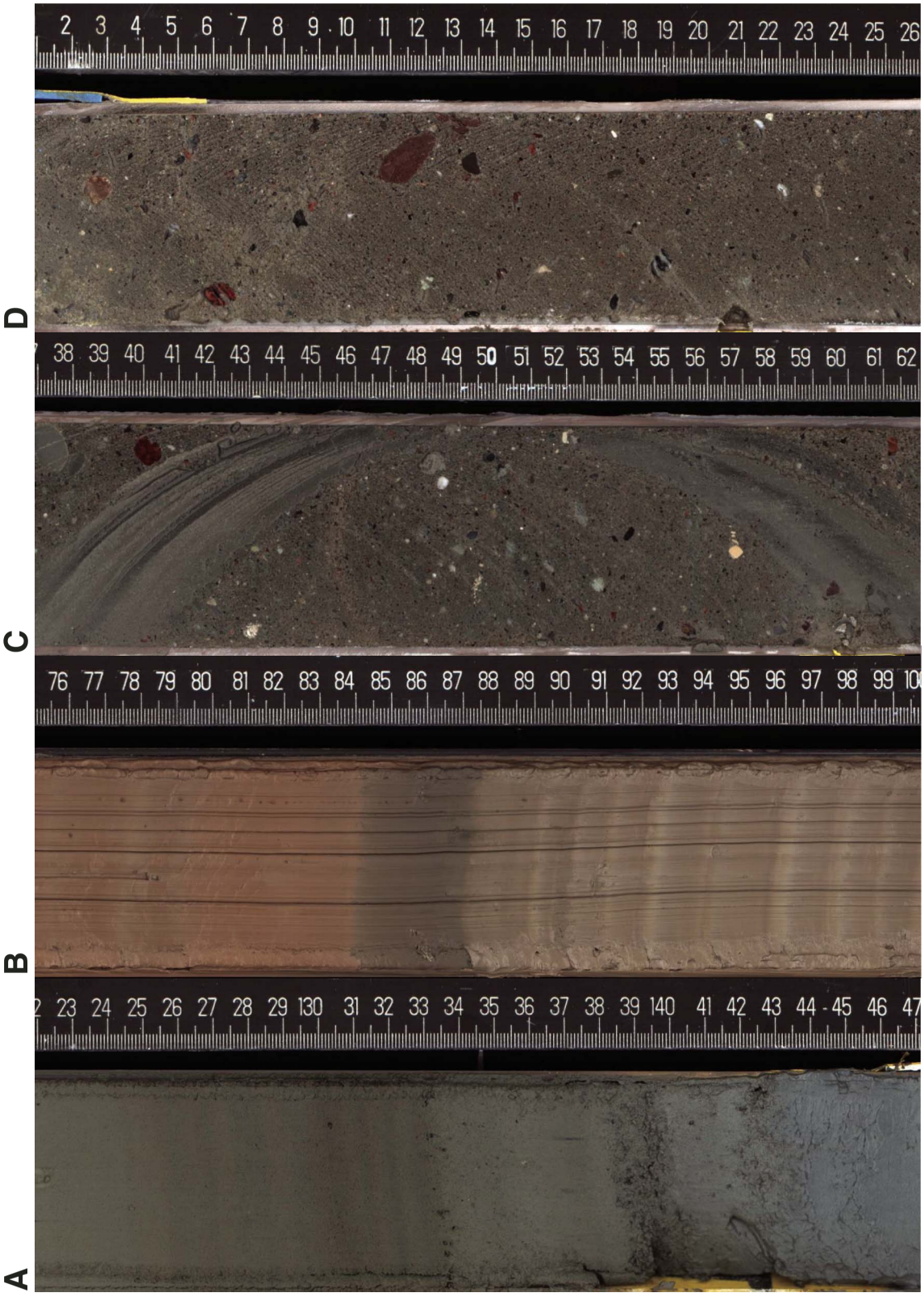

Figure F3. Line scan images of lithostratigraphic Units I–IV. The Unit I/II boundary is at 33 cm in the leftmost image from Core 347-M0064D-1H. **A.** Units I and II. **B.** Unit III. **C.** Subunit IVa. **D.** Subunit IVb.

Figure F4. Three reworked organic-walled dinoflagellate cysts from Core 347-M0064A-12H. **1.** *Apectodinium*. **2.** *Wetzeliella*. **3.** *Charlesdowniea*. Scale bars = 20 µm.

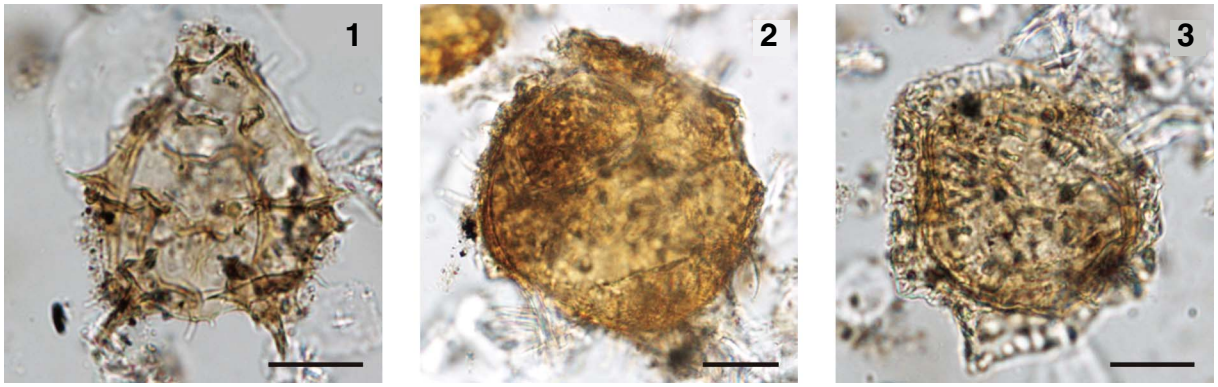

Figure F5. Concentrations of (**A**) chloride, (**B**) shipboard salinity calculated from refractive index, (**C**) chloride-based salinity, and (**D**) alkalinity in interstitial water samples, Site M0064.

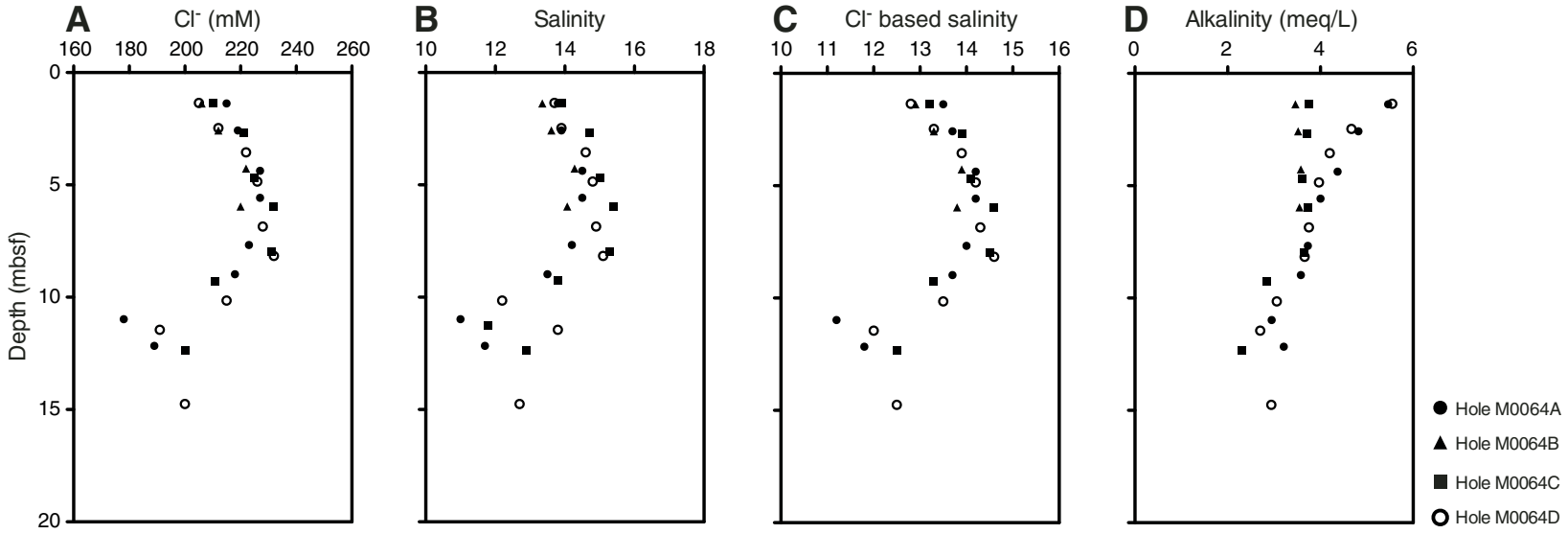

Figure F6. Concentrations and ratios of (**A**) sulfate, (**B**) sulfate/chloride, (**C**) ammonium, (**D**) phosphate, (**E**) iron, (**F**) manganese, and (**G**) pH from interstitial water samples, Site M0064. Dashed line = seawater ratio.

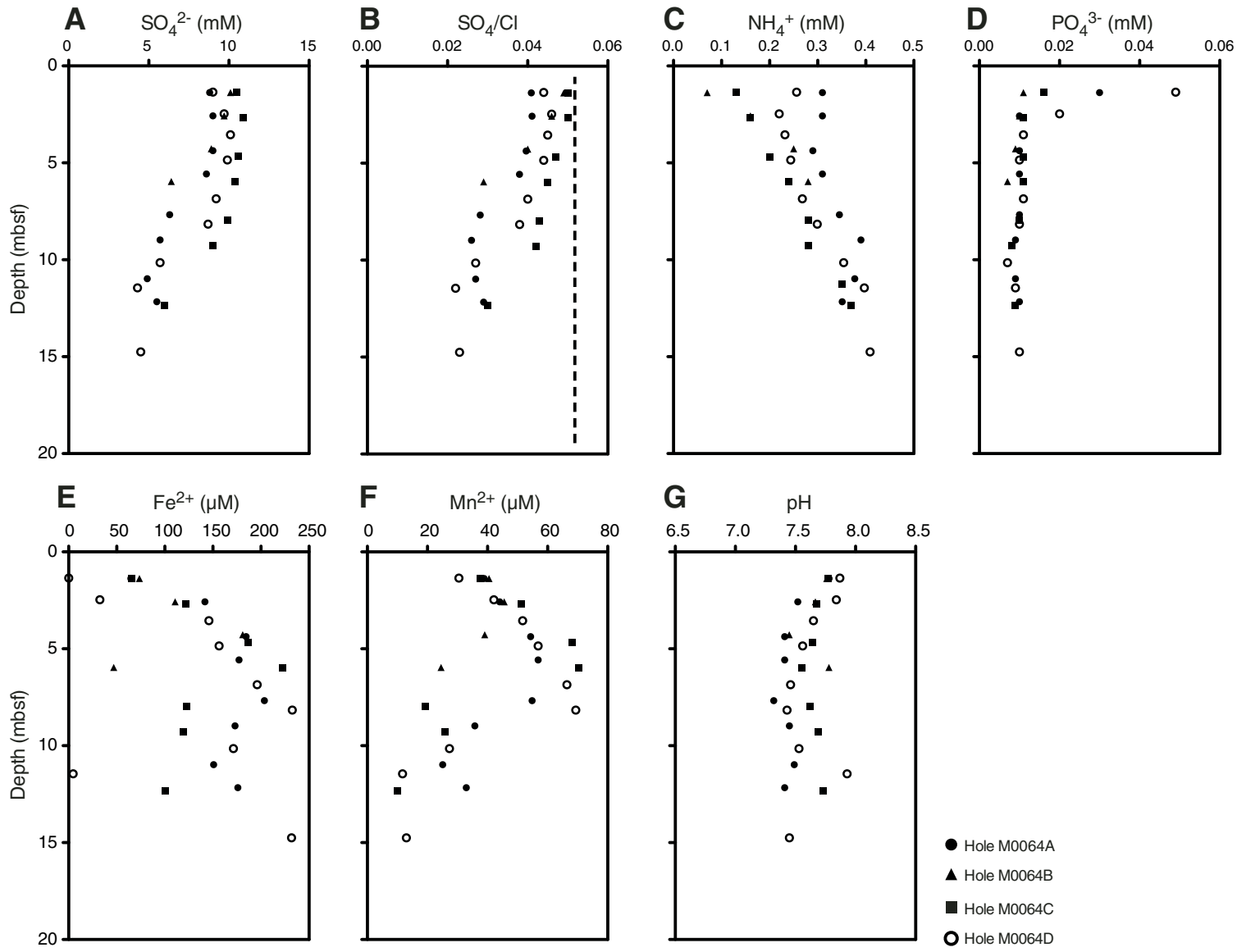

Figure F7. Concentrations and ratios of (**A**) bromide, (**B**) bromide/chloride, (**C**) boron, and (**D**) boron/chloride from interstitial water samples, Site M0064. Dashed lines = seawater ratio.

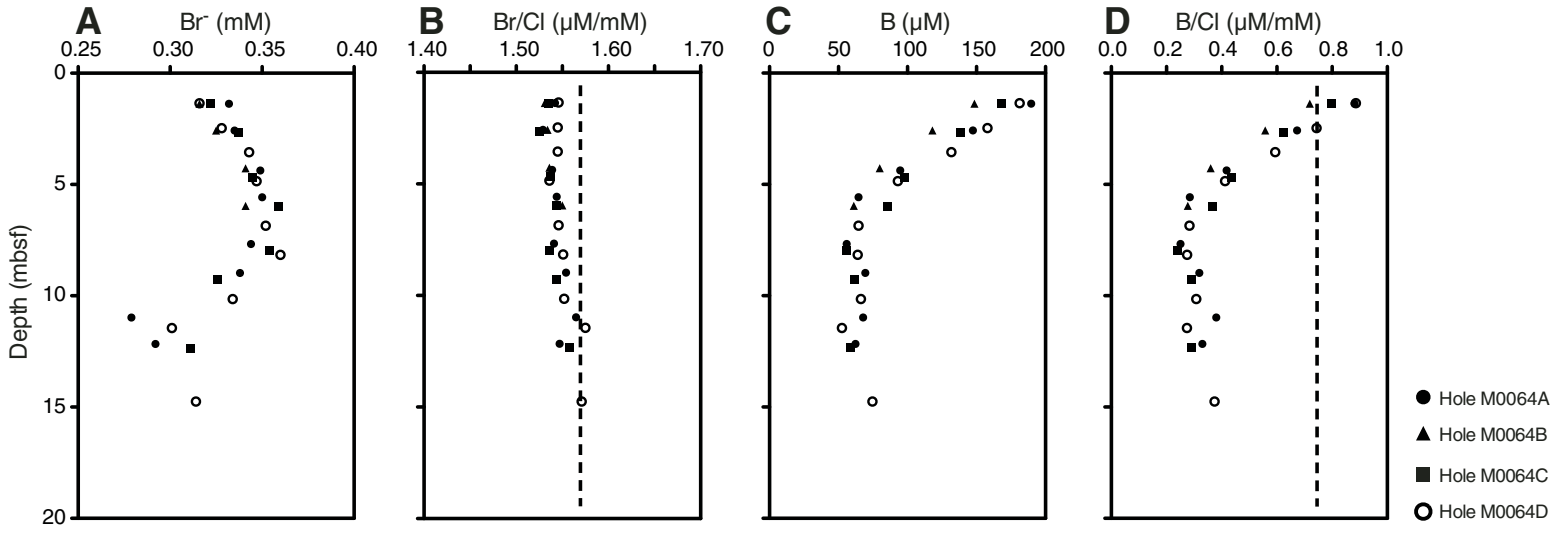

Figure F8. Concentrations and ratios of (**A**) sodium, (**B**) potassium, (**C**) magnesium, (**D**) calcium, (**E**) sodium/chloride, (**F**) potassium/chloride, (**G**) magnesium/chloride, and (**H**) calcium/chloride from interstitial water samples, Site M0064. Dashed lines = seawater ratio.

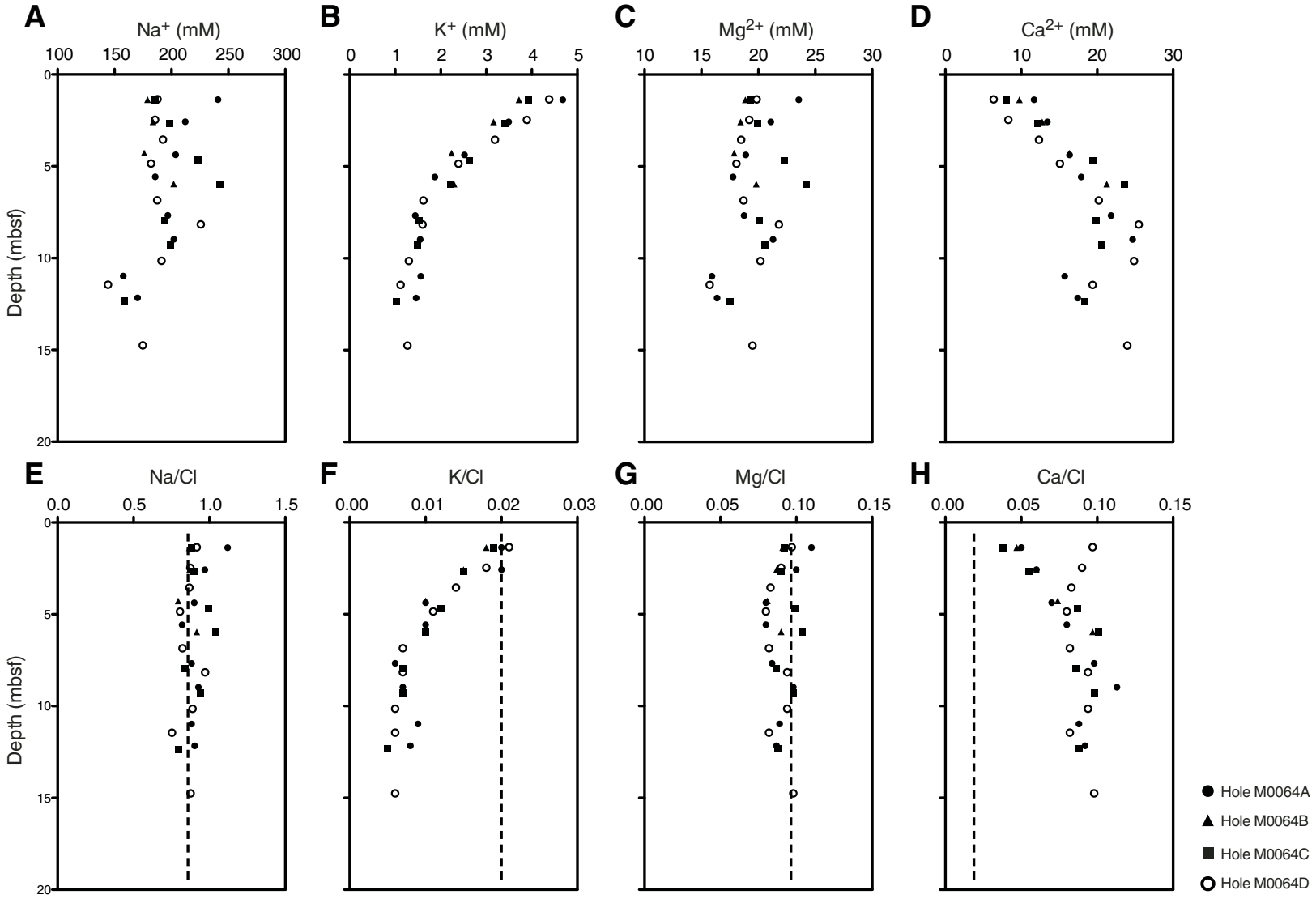

Figure F9. Concentrations of (**A**) strontium, (**B**) lithium, (**C**) dissolved silica, and (**D**) barium from interstitial water samples, Site M0064.

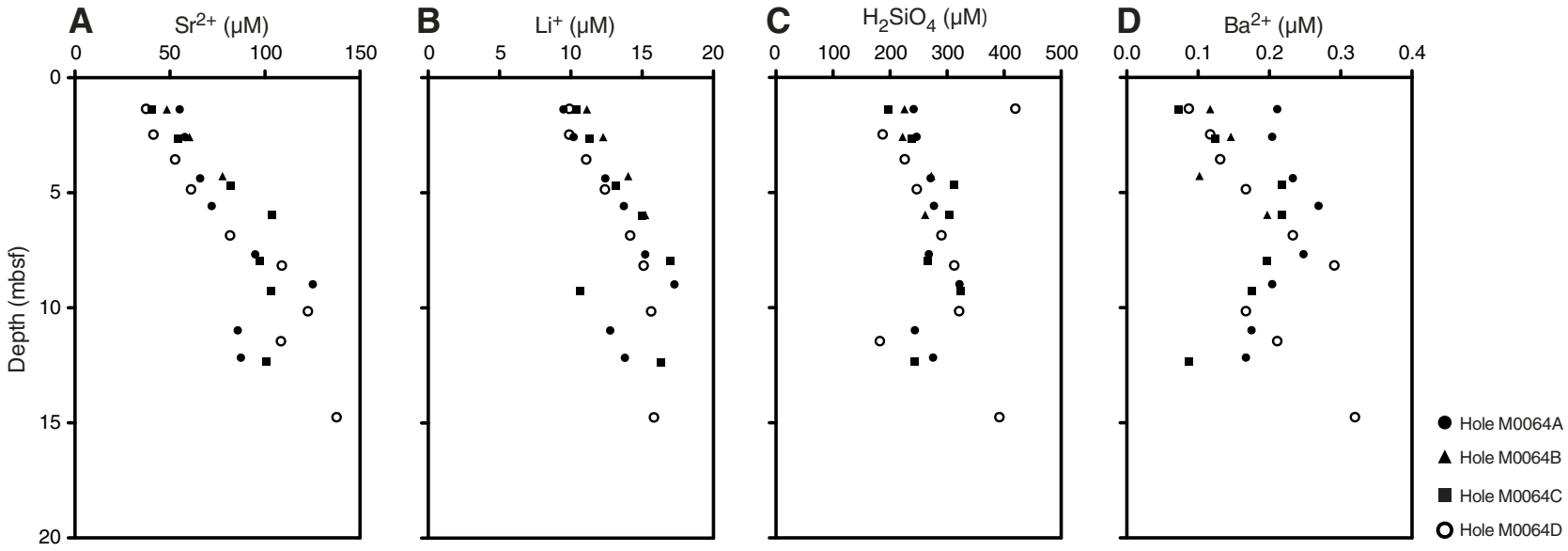

Figure F10. Sedimentary (**A**) total carbon (TC), (**B**) total organic carbon (TOC), (**C**) total inorganic carbon (TIC), and (**D**) total sulfur (TS) values, Site M0064.

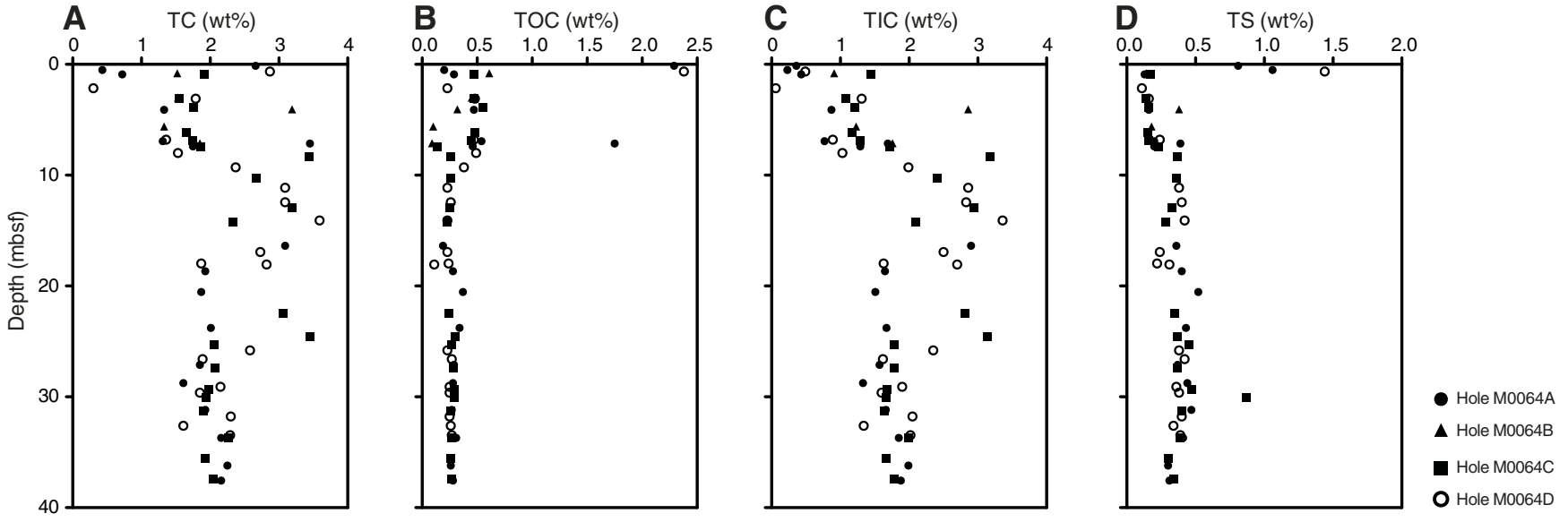

Figure F11. Natural gamma radiation (NGR) (cps), MSCL-measured magnetic susceptibility (MS) (10^{-5} SI), dry density (g/cm^3), and color reflectance parameter b*, Hole M0064A.

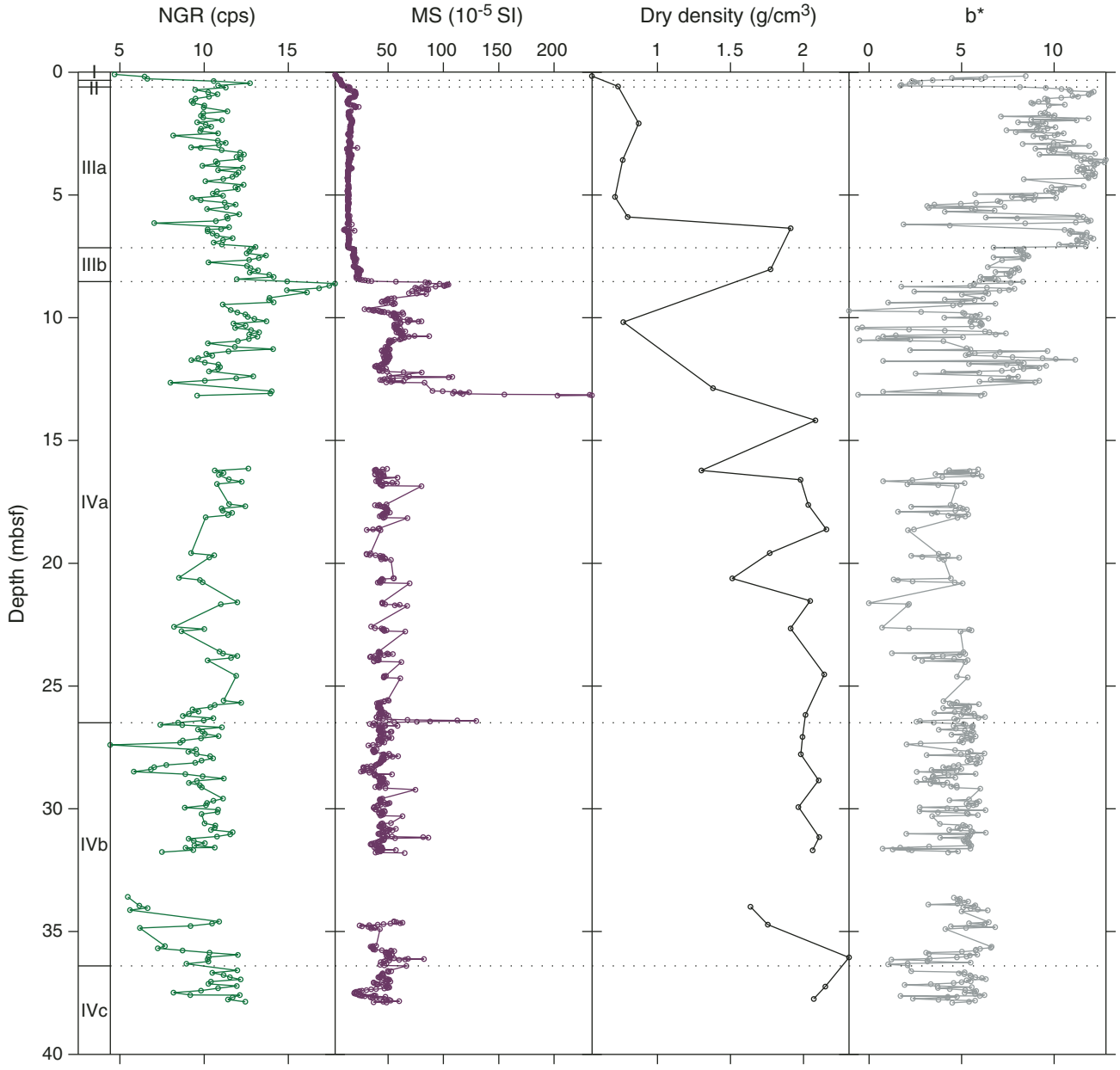

Figure F12. A. Gamma density (g/cm^3) and discrete bulk density (g/cm^3) measurements derived from pycnometer moisture and density analyses, Hole M0064A. **B.** Multisensor core logger (MSCL) *P*-wave and discrete velocity (m/s) measurements performed during the OSP, Hole M0064A.

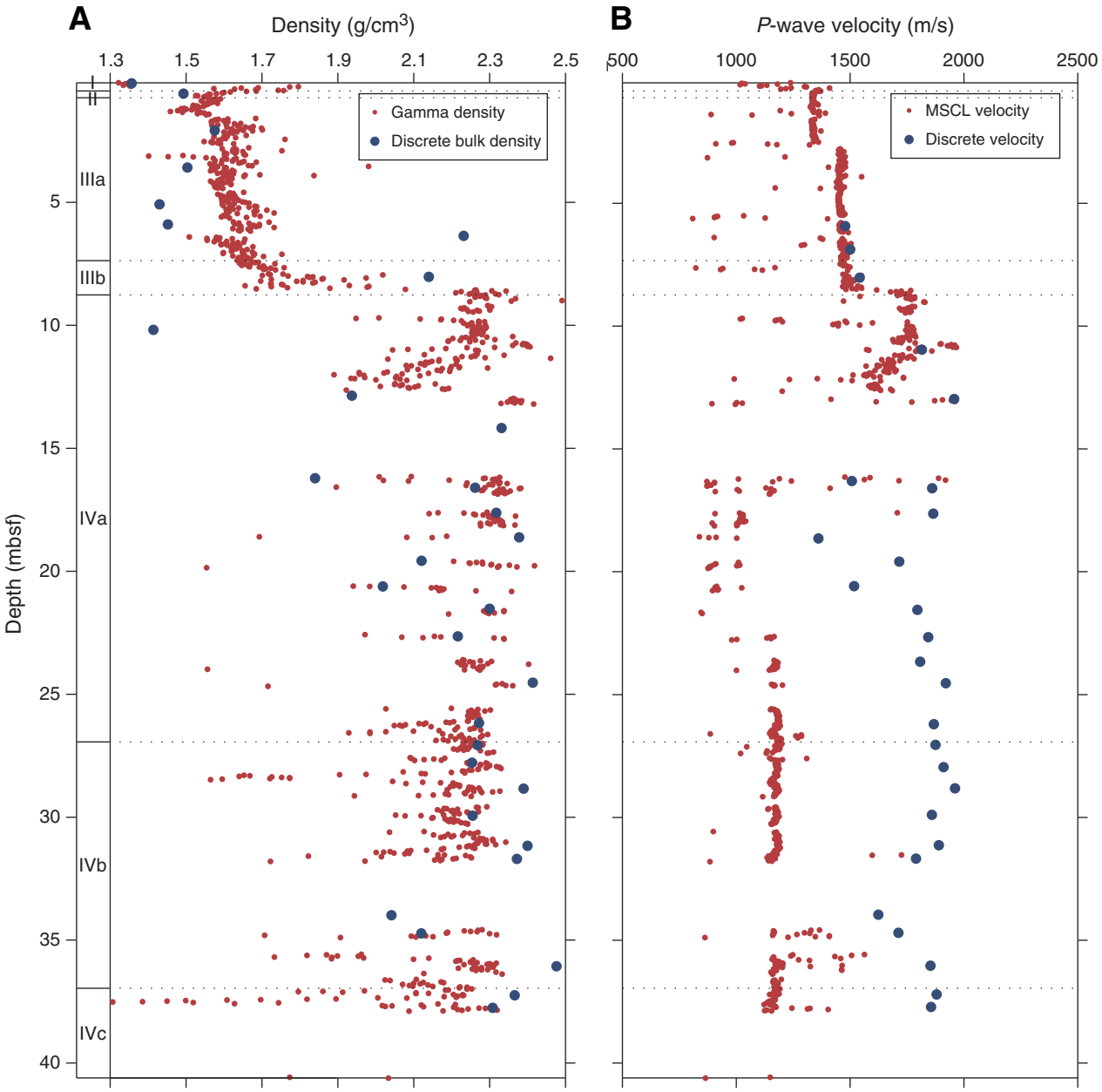

Figure F13. Plots and biplots of magnetic susceptibility (χ), natural remanent magnetization (NRM) intensity, and NRM inclination of discrete paleomagnetic samples, Hole M0064D. Dashed line = geocentric axial dipole (GAD) prediction of inclination for the site latitude. AF = alternating field.

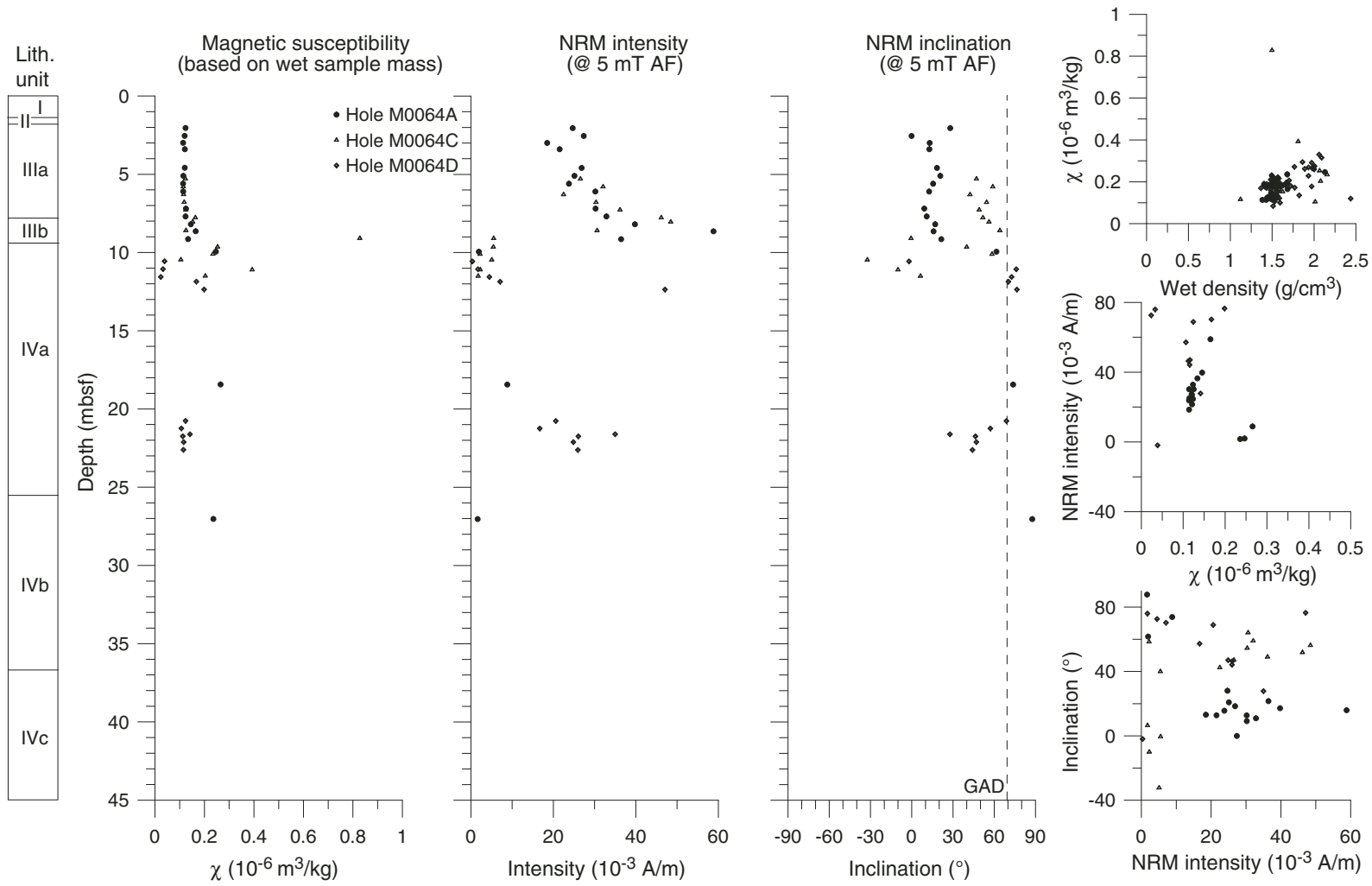

Figure F14. Plots of natural remanent magnetization (NRM) after alternating field (AF) demagnetization to 80 mT. A. Sample 347-M0064A-2H-2, 95 cm; 5.60 mbsf. B. Sample 347-M0064A-17H-1, 89 cm; 27.03 mbsf. Category 1 includes samples that do not contain a stable magnetization. Category 2 contains a vector that trends toward the origin during demagnetization. Open squares = vertical, solid squares = horizontal.

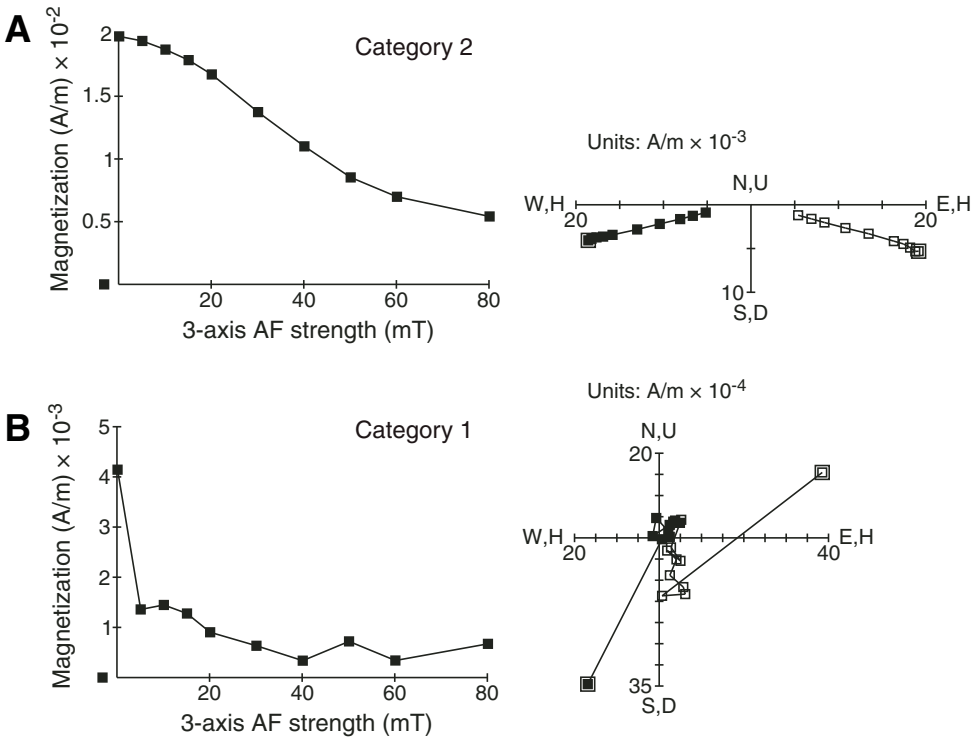

Figure F15. Plot of magnetic susceptibility (10^{-5} SI) data, Holes M0064A–M0064D.

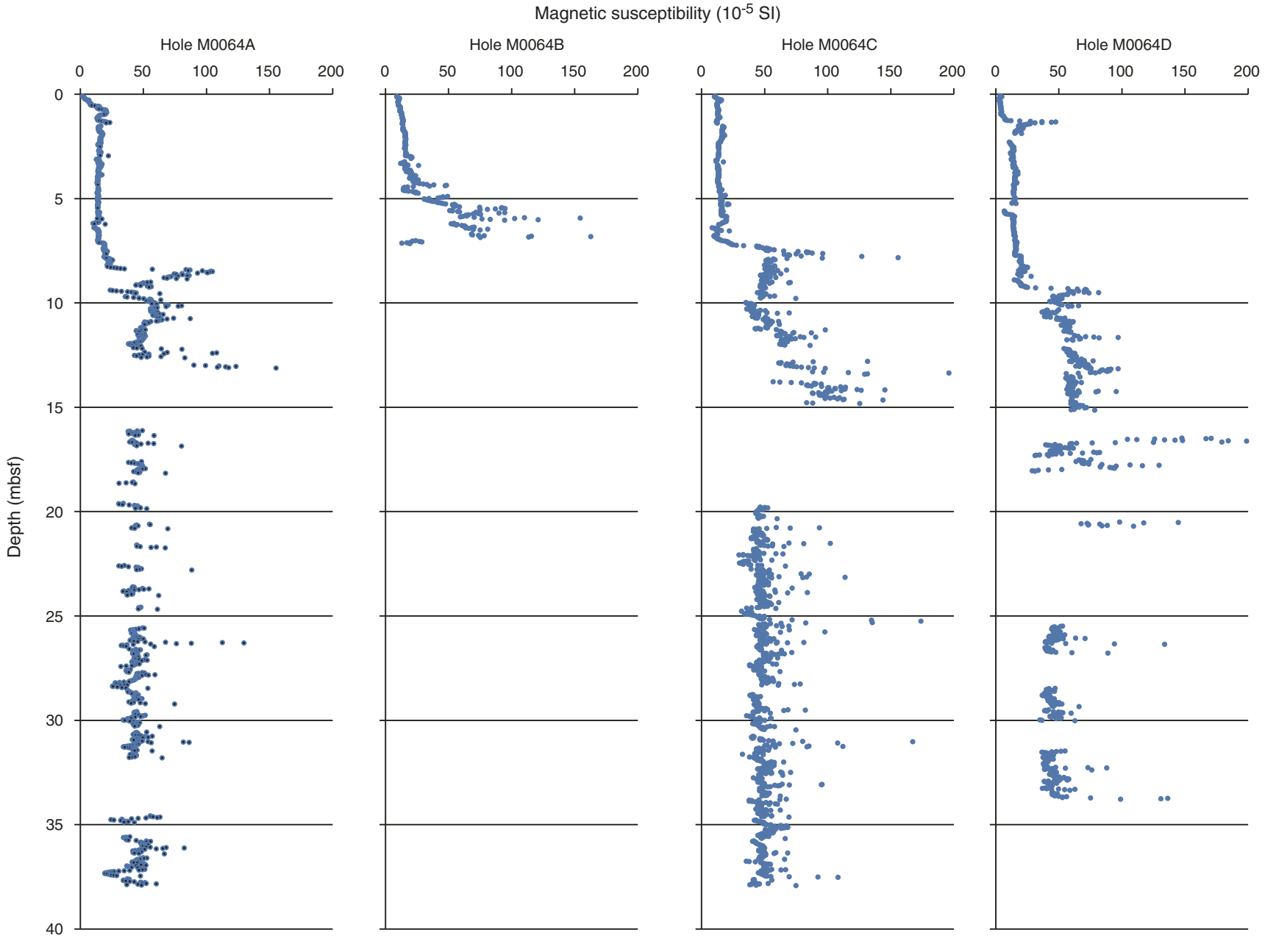

Figure F16. Correlation of the seismic profile with lithostratigraphic boundaries (seismic units and subunits) as well as multisensor core logger magnetic susceptibility data (Hole M0064A), Site M0064. SF = seafloor, BWT = bottom of Weichselian till, BR = bedrock.

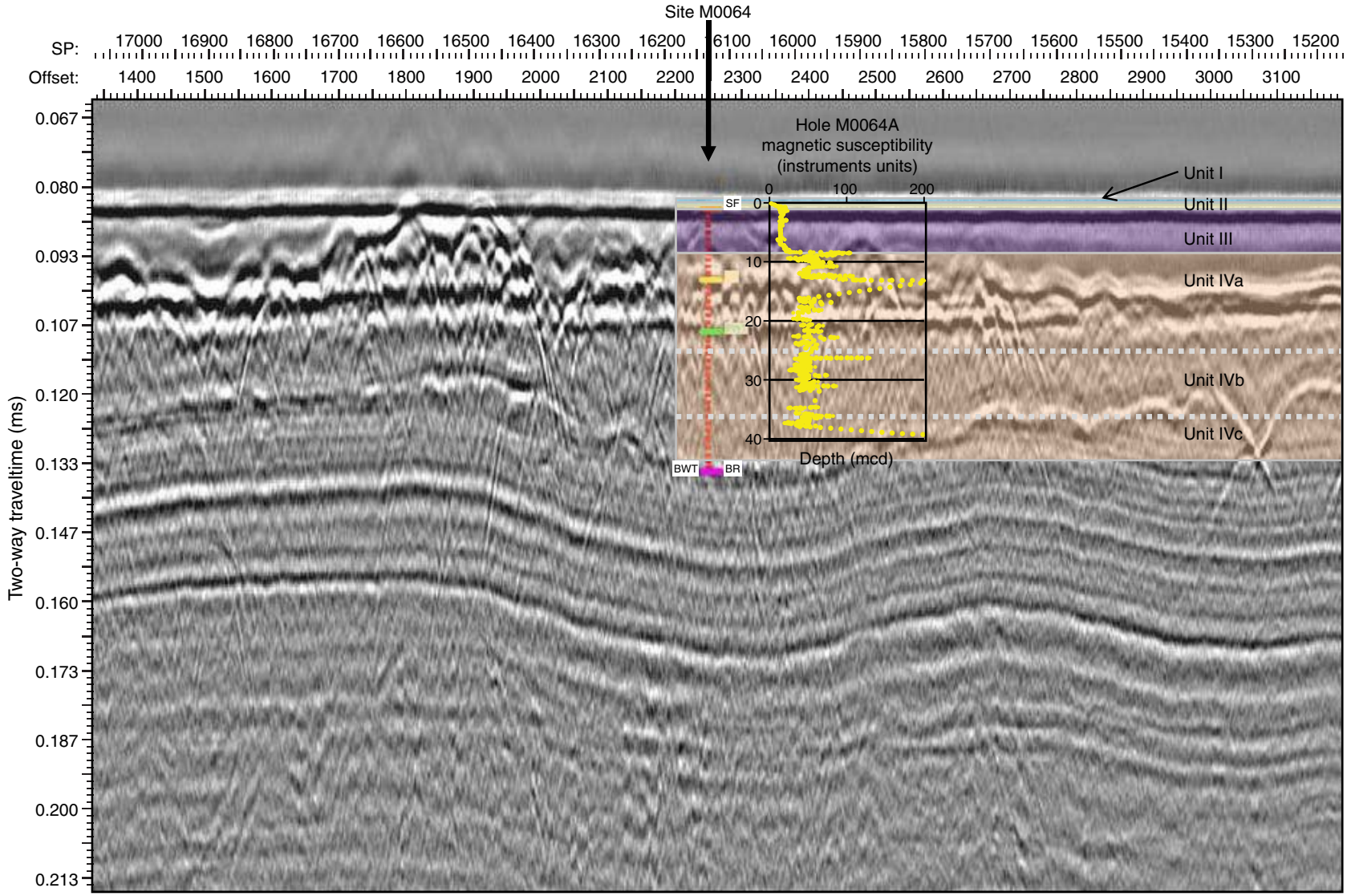

Figure F17. Gamma ray log, spectral gamma ray log, and resistivity log, Hole M0064D. The pipe was set at 7.6 m WSF.

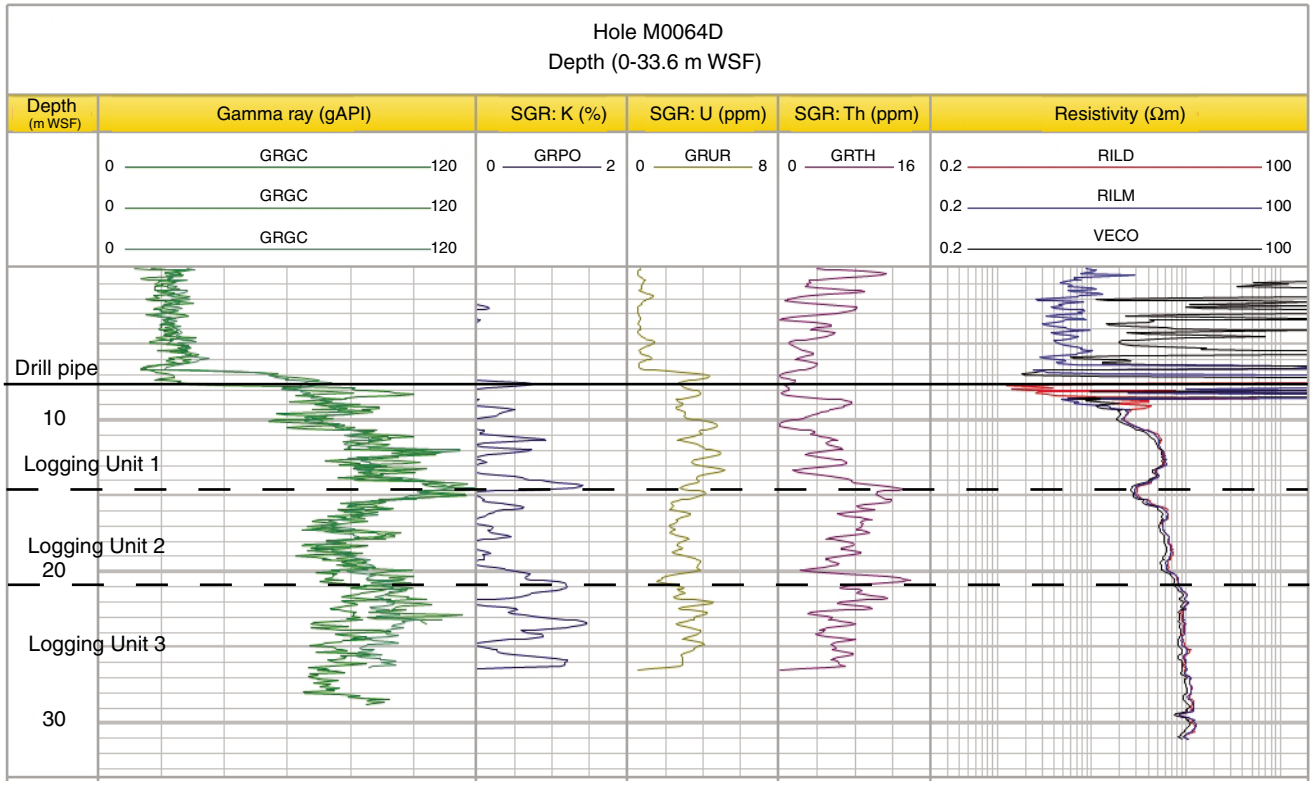

Table T1. Operations, Site M0064. (Continued on next two pages.)

Core	Coring method	Date (2013)	Time (UTC)	Depth (mbsf) Top	Depth (mbsf) Bottom	Recovered (m)	Recovery (%)	Mud type	Comments
347-M0064A-									
		20 Oct	1200						On Site M0064, prepared for ROV survey of seabed
		20 Oct	1245						Lowered template and ROV into moonpool
		20 Oct	1415						ROV survey of Holes M0064A–M0064C completed, ROV back on deck
		20 Oct	1425						Repositioned over Hole M0064A
1H	PCS	20 Oct	1545	0.00	3.00	3.32	110.67	Seawater	Fired from position calculated to be just above seabed
2H	PCS	20 Oct	1615	3.00	6.30	3.54	107.27	Seawater	
3H	PCS	20 Oct	1715	6.30	9.60	3.54	107.27	Seawater	
4H	PCS	20 Oct	1745	9.60	12.90	3.32	100.61	Seawater	Till
5N	NRCB	20 Oct	1845	12.90	15.90	0.60	20	Seawater	
6P	PCA	20 Oct	2000	15.90	16.05	0.15	100	Seawater	
7N	NRCB	20 Oct	2020	16.05	16.50	0.68	151.11	Guar	Basket catcher jammed with stones within till: removed for next run
8N	NRCB	20 Oct	2115	16.50	17.50	0.53	53	Guar	
9N	NRCB	20 Oct	2210	17.50	18.50	0.77	77	Guar	
10N	NRCB	20 Oct	2310	18.50	19.50	0.23	23	Guar	
11N	NRCB	20 Oct	2345	19.50	20.50	0.44	44	Guar	
12N	NRCB	21 Oct	0043	20.50	21.50	0.39	39	Guar	
13N	NRCB	21 Oct	0117	21.50	22.50	0.31	31	Guar	
14N	NRCB	21 Oct	0148	22.50	23.50	0.37	37	Guar	
15N	NRCB	21 Oct	0223	23.50	24.50	0.59	59	Guar	
16N	NRCB	21 Oct	0249	24.50	25.50	0.25	25	Guar	
17N	NRCB	21 Oct	0320	25.50	26.50	1.16	116	Guar	
18N	NRCB	21 Oct	0352	26.50	27.50	0.97	97	Guar	
19N	NRCB	21 Oct	0440	27.50	28.50	1.14	114	Guar	
20N	NRCB	21 Oct	0520	28.50	29.50	0.79	79	Guar	
21N	NRCB	21 Oct	0605	29.50	30.50	0.90	90	Guar	
22N	NRCB	21 Oct	0620	30.50	31.50	1.22	122	Guar	
23N	NRCB	21 Oct	0710	31.50	33.50	0.37	18.5	Guar	
24N	NRCB	21 Oct	0745	33.50	34.50	0.73	73	Guar	
25P	PCA	21 Oct	0841	34.50	35.50	0.44	44	Guar	
26N	NRCB	21 Oct	0910	35.50	36.50	0.95	95	Guar	
27N	NRCB	21 Oct	0940	36.50	37.50	1.21	121	Guar	
28N	NRCB	21 Oct	1015	37.50	38.50	0.45	45	Guar	Driller noted a change in drilling parameters within the last 20 cm
29N	NRCB	21 Oct	1110	38.50	39.50	0.00	0	Guar	PCD secondary bit lost two buttons and one partially lost
30N	NRCB	21 Oct	1150	39.50	40.50	0.00	0	Guar	Drilling like sand
31S	HS	21 Oct	1215	40.50	40.50	0.08		Guar	
32N	NRCB	21 Oct	1230	40.50	41.50	0.15	15	Guar	Chalk at base of run below more gravel
		21 Oct	1255						End of hole
		21 Oct	1315						Tripped pipe back to log hole
									Loggers unable to release brake on winch using ship's air supply; brake freed when ship increased air pressure
		21 Oct	1515						Abandoned logging attempt at this hole because ship required to change heading
		21 Oct	1520						Dismantled logging tools and exchanged coring tools in readiness for bumping over to Hole M0064B
347-M0064B-									
		21 Oct	1605						Completed bump over from Hole M0064A
1H	PCS	21 Oct	1615	0.00	3.30	3.46	104.85	Seawater	Water 1.22 m shallower than Hole M0064A
2H	PCS	21 Oct	1655	3.30	6.60	3.26	98.79	Seawater	~2 m of sand
3H	PCS	21 Oct	1735	6.60	7.10	0.32	64	Guar	Sand with gravel at base; no possibility of collecting material; open holed to penetrate expected 1.5 m
4O	NCA	21 Oct	1805	7.10	10.10	0.00	0	Guar	Open holed 3 m from last sample, drilling parameters suggest same or similar material as before
5S	HS	21 Oct	1825	10.10	10.20	0.10	100	Guar	Sand and gravel; this made 6 m of this material, and with the loss of 1 m when pulling back to take sample, decision made to end hole

Table T1 (continued). (Continued on next page.)

Core	Coring method	Date (2013)	Time (UTC)	Depth (mbsf) Top	Depth (mbsf) Bottom	Recovered (m)	Recovery (%)	Mud type	Comments
									Pulled pipe clear of seabed and bumped over to Hole M0064C
347-M0064C-									
		21 Oct	1915						Completed bump over from Hole M0064B
1H	PCS	21 Oct	1925	0.00	3.30	3.43	103.94	Seawater	
2H	PCS	21 Oct	2005	3.30	6.60	3.52	106.67	Seawater	Clay; mud valve stuck closed, several attempts to open; no pressure in string
3H	PCS	21 Oct	2050	6.60	9.90	3.33	100.91	Seawater	Slightly sandy clay
4H	PCS	21 Oct	2125	9.90	12.70	2.79	99.64	Seawater	65 bar but then rose to >100 bar; till at bottom of core
5N	NRCB	21 Oct	2220	12.70	13.70	0.78	78	Seawater	
6N	NRCB	21 Oct	2305	13.70	14.70	1.07	107	Seawater	
7N	NRCB	21 Oct	2330	14.70	15.70	0.24	24	Seawater	
8N	NRCB	21 Oct	2355	15.70	16.70	0.00	0	Seawater	No recovery, liner clean
9O	NCA	22 Oct	0020	16.70	18.70	0.00	0	Seawater	
10N	NRCB	22 Oct	0059	18.70	19.70	0.00	0	Seawater	No recovery, liner clean
11N	NRCB	22 Oct	0136	19.70	20.70	0.68	68	Seawater	
12N	NRCB	22 Oct	0214	20.70	21.70	1.34	134	Seawater	May have recovered end of previous run
13N	NRCB	22 Oct	0250	21.70	22.70	1.32	132	Seawater	
14N	NRCB	22 Oct	0317	22.70	23.70	1.43	143	Seawater	
15N	NRCB	22 Oct	0356	23.70	24.70	1.34	134	Seawater	
16N	NRCB	22 Oct	0443	24.70	25.70	1.20	120	Seawater	
17N	NRCB	22 Oct	0522	25.70	26.70	1.23	123	Seawater	
18N	NRCB	22 Oct	0600	26.70	27.70	1.53	153	Seawater	
19N	NRCB	22 Oct	0627	27.70	28.70	0.70	70	Seawater	
20N	NRCB	22 Oct	0652	28.70	29.70	1.23	123	Seawater	
21N	NRCB	22 Oct	0712	29.70	30.70	0.84	84	Seawater	
22N	NRCB	22 Oct	0753	30.70	31.70	1.23	123	Seawater	
23N	NRCB	22 Oct	0815	31.70	32.70	1.33	133	Seawater	
24N	NRCB	22 Oct	0840	32.70	33.70	1.50	150	Seawater	
25N	NRCB	22 Oct	0905	33.70	34.70	1.26	126	Seawater	
26N	NRCB	22 Oct	0935	34.70	35.70	1.30	130	Seawater	
27N	NRCB	22 Oct	1005	35.70	36.70	1.21	121	Seawater	
28N	NRCB	22 Oct	1035	36.70	37.70	1.48	148	Seawater	
29N	NRCB	22 Oct	1115	37.70	38.20	0.29	58	Seawater	
30S	HS	22 Oct	1148	38.20	38.20	0.04	0	Seawater	
31N	NRCB	22 Oct	1215	38.20	39.20	0.00	0	Seawater	
32N	NRCB	22 Oct	1310	39.20	40.20	0.00	0	Seawater	
33N	NRCB	22 Oct	1325	40.20	42.20	0.00	0	Seawater	
34N	NRCB	22 Oct	1355	42.20	43.20	0.02	2	Seawater	1 rounded pebble with a smearing of chalk recovered
35N	NRCB	22 Oct	1355	43.20	45.00	0.00	0	Seawater	
36S	HS	22 Oct	1445	45.00	45.10	0.10	100	Seawater	Granite and chalk recovered
									End of hole
		22 Oct	1505						Flushed borehole and carried out wiper trips while tripping pipe in preparation for logging
		22 Oct	1525						Hole collapsed from ~9 mbsf; attempted wiper trip unsuccessful; abandoned logging and prepared to bump over to Hole M0064D
347-M0064D-									
		22 Oct	1555						Completed bump over from Hole M0064C
1H	PCS	22 Oct	1625	0.00	2.20	3.02	137.27	Seawater	43 bar; this sea surface sample was the first aromatic core at this location
2H	PCS	22 Oct	1700	2.20	5.50	3.50	106.06	Seawater	50 bar
3H	PCS	22 Oct	1740	5.50	8.80	3.54	107.27	Seawater	68 bar
4H	PCS	22 Oct	1819	8.80	12.10	3.47	105.15	Seawater	100 bar, took a second attempt to fall to zero; soft diamicton, attempted another piston
5H	PCS	22 Oct	1859	12.10	15.40	3.69	111.82	Seawater	Fired at 62 bar, dropped to 50 bar, rose to 100 bar; spline + 2 rings came off overshot release tool; spline was fished with the magnet and rings recovered; soft diamicton recovered; swap to NRCB for next run

Table T1 (continued).

Core	Coring method	Date (2013)	Time (UTC)	Depth (mbsf) Top	Depth (mbsf) Bottom	Recovered (m)	Recovery (%)	Mud type	Comments
6N	NRCB	22 Oct	2025	15.40	16.40	0.00	0	Guar	Possibly did not latch in correctly
7N	NRCB	22 Oct	2050	16.40	17.40	1.36	136	Guar	Hard diamicton
8N	NRCB	22 Oct	2130	17.40	18.20	0.71	88.75	Guar	
9N	NRCB	22 Oct	2213	18.20	19.20	0.00	0	Guar	
10N	NRCB	22 Oct	2330	19.20	20.40	0.00	0	Guar	Possibly did not latch in properly
11N	NRCB	23 Oct	0015	20.40	21.40	0.35	35	Guar	
12N	NRCB	23 Oct	0045	21.40	22.40	0.20	20	Guar	
13N	NRCB	23 Oct	0110	22.40	23.40	0.00	0	Guar	
14O	NCA	23 Oct	0145	23.40	25.40	0.00	0	Guar	Inserted bit to clear blockage
15N	NRCB	23 Oct	0218	25.40	26.40	1.15	115	Guar	
16N	NRCB	23 Oct	0245	26.40	27.40	0.50	50	Guar	
17O	NCA	23 Oct	0315	27.40	28.40	0.00	0	Guar	Inserted bit used to clear stone in throat of drill bit
18N	NRCB	23 Oct	0329	28.40	29.40	1.44	144	Guar	Reran NRC for core run; left on a badly worn bit (with a good inside gauge) because stone expected; good core recovered and bit still usable
19N	NRCB	23 Oct	0356	29.40	30.40	0.66	66	Guar	
20O	NCA	23 Oct	0415	30.40	31.40	0.00	0	Guar	Ran insert bit to dig and remove suspected stone in front of bit
21N	NRCB	23 Oct	0450	31.40	32.40	1.43	143	Guar	Gritty clay core recovered
22N	NRCB	23 Oct	0522	32.40	33.40	1.3	130	Guar	
23N	NRCB	23 Oct	0544	33.40	33.90	0.44	88	Guar	Unable to core 1 m, so stopped to retrieve NRCB and set up for NCA to 41 mbsf
24O	NCA	23 Oct	0625	33.90	41.00	0.00	0	Guar	Rooster box down at deck level; pulled NCA and prepared to take hammer sample to prove ground
25S	HS	23 Oct	0740	41.00	41.20	0.20	100	Guar	Pea-size gravel recovered
		23 Oct	0755						End of hole
		23 Oct	0755						Circulated mud; set up logging gear on deck while circulating
		23 Oct	0810						Commenced tripping pipe to 10 mbsf
		23 Oct	0902						Logging tool reached 31 mbsf
		23 Oct	0931						Second string of tools ran in compensation, reached 21 mbsf only; decided not to run third string
		23 Oct	1000						Dismantled logging deck and prepared to trip pipe
		23 Oct	1015						Tripped pipe
		23 Oct	1050						BHA in slips
		23 Oct	1050						Lifted template
		23 Oct	1105						Cleaned template of cuttings in moonpool
		23 Oct	1120						Template on deck

HS = hammer sampler, NCA = noncoring assembly, NRCB = nonrotating core barrel, PCA = push coring assembly, PCS = piston coring system. ROV = remotely operated vehicle, PCD = polycrystalline diamond, BHA = bottom-hole assembly.

Table T2. Diatoms, Hole M0064A.

Affinity	Life form	Diatoms	Depth (mbsf): 0 Core, section: 1H-1	6.3 3H-1 Barren
BM	Pelagic	*Actinocyclus octonarius* Ehrenberg	x	
BF	Pelagic	*Actinocyclus octonarius* var. *crassus* (W. Smith) Hendey	x	
BM	Pelagic	*Chaetoceros* resting spores spp.	x	
BM	Pelagic	*Chaetoceros* spp. vegetative cells	x	
B	Epiphytic	*Cocconeis scutellum* Ehrenberg	x	
B	Pelagic	*Coscinodiscus granii* Gough	x	
B	Pelagic and epilithic	*Cyclotella choctawhatcheeana* Prasad	x	
BF	Epiphytic	*Epithemia turgida* (Ehrenberg) Kützing	x	
BM	Epiphytic	*Grammatophora oceanica* Ehrenberg	x	
M	Epiphytic	*Hyalodiscus scoticus* (Kützing) Grunow	x	
B	Pelagic and on ice	*Melosira arctica* Dickie	x	
B	Pelagic and ice	*Pauliella taeniata* (Grunow) Round and Basson	x	
M	Pelagic	*Pseudosolenia calcar-avis* (Schultze) B.G. Sundström	x	
B	Epiphytic and epilithic	*Rhoicosphenia curvata (*Kützing) Grunow	x	
B	Pelagic	*Thalassiosira hyperborea* var. *lacunosa* (Berg) Hasle	x	
B	Pelagic	*Thalassiosira levanderi* Van Goor	x	
		Crysophyte cysts		
		Smooth	x	
		With curves	x	
		Dots		

BF = brackish-freshwater, B = brackish, BM = brackish-marine, M = marine. x = present.

Table T3. Interstitial water geochemistry, Site M0064.

Core, section, interval (cm)	Type	Depth (mbsf)	Volume (mL)	Analyte:	pH	Salinity	Alkalinity	Cl^-	Br^-	SO_4^{2-}	H_2S	NH_4^+	Na^+	K^+	Mg^{2+}	Ca^{2+}	Sr^{2+}	Li^+	H_4SiO_4	Ba^{2+}	B	Al	PO_4^{3-}	Fe^{2+}	Mn^{2+}
				Unit:			meq/L	mM	mM	mM	mM	mM	mM	mM	mM	mM	µM	µM	µM	µM	µM	µM	mM	µM	µM
				Method:	ISE	Refraction	Titration	IC	IC	IC	Photometrical	Conductivity	ICP-OES	ICP-OES	ICP-OES	ICP-OES	ICP-OES	ICP-OES	ICP-OES	ICP-OES	ICP-OES	ICP-OES	ICP-OES	ICP-OES	ICP-OES
347-M0064A-																									
1H-1, 135–140	Rh	1.38	16.00		7.78	13.80	5.46	215.14	0.33	8.80	—	0.31	240.84	4.68	23.55	11.68	55.09	9.49	241.27	0.21	189.62	0.93	0.03	64.64	38.88
1H-2, 105–110	Rh	2.58	11.00		7.52	13.90	4.82	219.05	0.34	9.00	—	0.31	212.14	3.49	21.09	13.43	57.74	10.19	246.54	0.20	147.44	2.22	0.01	141.71	44.03
2H-1, 135–140	Rh	4.38	13.50		7.41	14.50	4.37	226.84	0.35	8.99	—	0.29	203.65	2.52	18.89	16.37	65.85	12.42	271.32	0.23	94.72	3.19	0.01	184.62	54.36
2H-2, 105–110	Rh	5.58	11.50		7.41	14.50	4.00	226.95	0.35	8.62	—	0.31	185.78	1.87	17.78	17.90	71.96	13.72	277.02	0.27	64.56	0.78	0.01	177.15	56.85
3H-1, 135–140	Rh	7.68	10.00		7.32	14.20	3.73	222.94	0.34	6.28	—	0.35	196.82	1.44	18.75	21.83	94.92	15.21	268.11	0.25	55.87	0.33	0.01	203.60	54.82
3H-2, 115–120	Rh	8.98	13.00		7.45	13.50	3.58	217.73	0.34	5.75	—	0.39	202.13	1.55	21.29	24.66	125.20	17.27	321.70	0.20	69.37	0.30	0.01	173.09	35.76
4H-1, 135–140	Rh	10.98	11.00		7.49	11.00	2.95	178.39	0.28	4.88	—	0.38	157.59	1.56	15.92	15.71	85.64	12.77	243.48	0.17	67.80	3.56	0.01	150.79	25.08
4H-2, 104–109	Rh	12.17	10.50		7.41	11.70	3.21	188.56	0.29	5.46	—	0.35	170.33	1.46	16.38	17.44	87.32	13.79	275.45	0.17	62.25	0.74	0.01	175.92	32.94
347-M0064B-																									
1H-1, 135–140	Rh	1.38	11.50		7.76	13.35	3.46	206.34	0.32	10.08	—	0.07	179.03	3.72	18.86	9.76	48.36	11.14	225.35	0.12	148.46	3.15	0.01	73.54	40.50
1H-2, 105–110	Rh	2.58	8.50		7.67	13.61	3.52	211.61	0.32	9.75	—	0.16	183.82	3.16	18.44	12.76	60.25	12.27	222.11	0.15	118.03	0.33	0.01	110.72	45.54
2H-1, 95–100	Rh	4.28	32.00		7.45	14.28	3.58	221.76	0.34	8.92	—	0.25	176.12	2.24	17.88	16.32	77.66	14.03	272.28	0.10	79.83	0.44	0.01	181.04	39.07
2H-2, 114–119	Rh	5.97	20.00		7.78	14.07	3.55	220.19	0.34	6.40	—	0.28	202.00	2.29	19.82	21.26	103.72	15.21	261.56	0.20	61.05	3.11	0.01	46.86	24.52
347-M0064C-																									
1H-1, 135–140	Rh	1.38	15.00		7.77	13.90	3.76	210.02	0.32	10.53	—	0.13	185.56	3.92	19.31	7.99	40.42	10.37	197.01	0.07	167.88	1.59	0.02	65.63	37.68
1H-2, 114–119	Rh	2.67	10.00		7.68	14.70	3.71	220.92	0.34	10.94	—	0.16	198.52	3.41	19.95	12.16	54.11	11.34	238.67	0.12	138.10	0.33	0.01	121.48	51.14
2H-1, 135–140	Rh	4.68	8.00		7.64	15.00	3.61	224.52	0.35	10.56	—	0.20	223.49	2.62	22.28	19.45	81.77	13.18	312.55	0.22	97.49	3.41	0.01	186.77	68.18
2H-2, 115–120	Rh	5.98	12.00		7.55	15.40	3.74	232.43	0.36	10.41	—	0.24	242.63	2.21	24.19	23.56	103.86	15.03	303.93	0.22	85.47	0.44	0.01	222.22	70.37
3H-1, 135–140	Rh	7.98	16.00		7.62	15.30	3.64	230.70	0.35	9.93	—	0.28	193.87	1.52	20.10	19.87	97.48	16.99	266.80	0.20	55.41	0.00	0.01	122.75	19.35
3H-2, 115–120	Rh	9.28	3.00		7.69	13.80	2.85	211.29	0.33	8.97	—	0.28	199.13	1.49	20.60	20.66	103.32	10.69	324.19	0.17	61.33	0.48	0.01	119.22	25.74
4H-1, 135–140	Rh	11.28	1.00		—	11.80	—	—	—	—	—	0.35	—	—	—	—	—	—	—	—	—	—	—	—	—
4H-2, 92–97	Rh	12.35	3.00		7.73	12.90	2.31	199.74	0.31	5.99	—	0.37	158.63	1.02	17.55	18.35	100.75	16.32	242.34	0.09	58.37	7.23	0.01	100.60	10.04
347-M0064D-																									
1H-1, 130–135	Rh	1.35	21.00		7.87	13.70	5.55	204.72	0.32	8.95	—	0.26	187.73	4.38	19.85	6.36	37.40	9.91	419.80	0.09	181.30	0.26	0.05	0.00	30.48
1H-2, 92–97	Rh	2.47	13.00		7.84	13.90	4.67	212.48	0.33	9.71	—	0.22	185.69	3.89	19.20	8.30	41.29	9.89	187.04	0.12	157.99	0.52	0.02	32.45	42.09
2H-1, 130–135	Rh	3.55	12.00		7.65	14.60	4.20	221.76	0.34	10.06	—	0.23	192.47	3.19	18.49	12.33	52.72	11.08	225.60	0.13	131.81	0.48	0.01	145.85	51.67
2H-2, 110–115	Rh	4.85	10.00		7.56	14.80	3.97	225.84	0.35	9.89	—	0.24	182.04	2.39	18.07	15.09	61.06	12.39	246.82	0.17	93.05	0.44	0.01	156.49	56.85
3H-1, 130–135	Rh	6.85	9.50		7.46	14.90	3.75	227.98	0.35	9.19	—	0.27	187.52	1.62	18.70	20.22	81.64	14.16	290.12	0.23	64.56	0.44	0.01	196.08	66.42
3H-2, 111–116	Rh	8.16	10.00		7.43	15.10	3.66	232.37	0.36	8.73	—	0.30	225.79	1.60	21.80	25.48	108.89	15.11	312.59	0.29	63.92	0.89	0.01	232.61	69.39
4H-1, 130–135	Rh	10.15	6.50		7.53	12.20	3.06	215.04	0.33	5.72	—	0.35	191.26	1.30	20.18	24.86	122.57	15.63	321.06	0.17	66.23	1.30	0.01	171.37	27.35
4H-2, 110–115	Rh	11.45	2.30		7.93	13.80	2.70	191.48	0.30	4.29	—	0.40	144.32	1.12	15.73	19.41	108.45	—	182.16	0.21	52.54	0.44	0.01	4.71	11.71
5H-1, 130–135	Rh	13.45	0.00		—	—	—	—	—	—	—	—	—	—	—	—	—	—	—	—	—	—	—	—	—
5H-2, 110–115	Rh	14.75	6.50		7.45	12.70	2.94	199.59	0.31	4.51	—	0.41	174.77	1.27	19.49	23.96	137.75	15.83	391.67	0.32	74.55	1.63	0.01	231.89	12.99
Reference samples																									
R2 salt brine mud 1	—	—	—		7.45	170.07	2.35	3448.94	0.00	17.47	0.00	0.00	3372.77	5.85	14.36	12.48	420.57	6.06	35.78	8.98	137.36	0.22	0.01	13.54	6.46
R3 seawater from mud pump	—	—	—		7.69	16.87	2.14	265.91	0.33	11.68	0.00	0.00	254.37	4.99	23.53	5.07	45.41	11.86	7.62	3.18	187.77	0.56	0.01	0.00	2.87
R4 grease 1 drill pipe	—	—	—		6.28	2.56	0.26	0.18	0.00	0.01	0.00	0.02	0.00	0.00	0.00	0.01	0.13	1.18	0.57	4.69	8.69	0.00	0.01	0.00	2.86
R5 grease 2 pipes	—	—	—		6.51	3.04	0.27	0.09	0.00	0.00	0.00	0.02	0.00	0.00	0.00	0.04	0.08	0.29	0.00	4.05	6.94	0.00	0.01	0.00	2.86
R6 grease 3 core barrel	—	—	—		6.54	4.49	0.26	0.08	0.00	0.00	0.00	0.03	0.00	0.00	0.00	0.03	0.07	0.29	1.53	3.90	6.47	0.00	0.01	0.00	2.86
R7 grease 4 “moly” piston rod grease	—	—	—		4.34	0.00	0.11	0.05	0.00	0.00	0.00	0.00	0.00	0.00	0.00	0.00	0.01	0.41	0.00	0.43	5.09	0.00	0.01	0.00	2.86
R8 grease 5 pipe thread	—	—	—		6.30	5.56	0.23	0.39	0.00	0.03	0.00	0.03	0.00	0.00	0.00	0.00	0.05	1.57	0.61	3.01	6.94	0.00	0.01	0.00	2.86
R9 tap water GC	—	—	—		6.49	0.00	0.26	5.06	0.01	0.04	0.00	0.00	4.65	0.14	0.05	0.03	0.24	0.90	7.23	8.71	104.80	0.22	0.01	0.00	2.89
R10 H_2Od ELGA	—	—	—		6.21	0.00	0.35	0.06	0.00	0.00	0.00	0.00	0.00	0.00	0.00	0.00	0.01	0.38	0.53	1.30	9.99	0.37	0.01	0.00	2.86
R11 mud 2 (GS550)	—	—	—		7.74	41.48	9.62	643.71	0.49	20.60	0.00	1.36	807.31	9.05	41.80	8.83	98.60	19.35	23.11	1.69	343.63	1.63	0.01	8.99	5.15
R12 mud 3 (guar gum)	—	—	—		6.40	16.60	2.20	239.64	0.36	12.35	0.00	0.07	223.23	5.61	24.40	4.91	36.57	12.51	8.47	1.94	192.03	0.37	0.01	0.00	3.02
R13 seawater/drill water	—	—	—		7.83	14.94	2.21	241.08	0.36	8.87	0.00	0.00	216.62	5.09	24.56	4.96	37.02	12.67	5.70	1.88	190.27	0.00	0.01	0.56	2.93
R26 M0064/surface seawater	—	—	—		7.76	6.54	1.85	113.81	0.17	5.96	0.00	0.00	103.57	2.36	11.62	2.79	18.63	5.17	6.94	0.02	88.34	0.15	0.01	0.00	2.87

Rh = Rhizon sample. ISE = ion-specific electrode, IC = ion chromatography, ICP-OES = inductively coupled plasma–optical emission spectroscopy. — = no data reported for samples with insufficient pore water volumes.

Table T4. Calculated salinity and elemental ratios of interstitial waters, Site M0064.

Core, section, interval (cm)	Type	Depth (mbsf)	Cl^- based salinity	Na/Cl (mM/mM)	Ca/Cl (mM/mM)	Mg/Cl (mM/mM)	K/Cl (mM/mM)	Br/Cl (µM/mM)	B/Cl (µM/mM)	SO_4/Cl (mM/mM)
347-M0064A-										
1H-1, 135–140	Rh	1.38	13.5	1.12	0.05	0.11	0.02	1.54	0.88	0.041
1H-2, 105–110	Rh	2.58	13.7	0.97	0.06	0.10	0.02	1.53	0.67	0.041
2H-1, 135–140	Rh	4.38	14.2	0.90	0.07	0.08	0.01	1.54	0.42	0.040
2H-2, 105–110	Rh	5.58	14.2	0.82	0.08	0.08	0.01	1.54	0.28	0.038
3H-1, 135–140	Rh	7.68	14.0	0.88	0.10	0.08	0.01	1.54	0.25	0.028
3H-2, 115–120	Rh	8.98	13.7	0.93	0.11	0.10	0.01	1.55	0.32	0.026
4H-1, 135–140	Rh	10.98	11.2	0.88	0.09	0.09	0.01	1.57	0.38	0.027
4H-2, 104–109	Rh	12.17	11.8	0.90	0.09	0.09	0.01	1.55	0.33	0.029
347-M0064B-										
1H-1, 135–140	Rh	1.38	12.9	0.87	0.05	0.09	0.02	1.53	0.72	0.049
1H-2, 105–110	Rh	2.58	13.3	0.87	0.06	0.09	0.01	1.53	0.56	0.046
2H-1, 95–100	Rh	4.28	13.9	0.79	0.07	0.08	0.01	1.54	0.36	0.040
2H-2, 114–119	Rh	5.97	13.8	0.92	0.10	0.09	0.01	1.55	0.28	0.029
347-M0064C-										
1H-1, 135–140	Rh	1.38	13.2	0.88	0.04	0.09	0.02	1.53	0.80	0.050
1H-2, 114–119	Rh	2.67	13.9	0.90	0.06	0.09	0.02	1.53	0.63	0.050
2H-1, 135–140	Rh	4.68	14.1	1.00	0.09	0.10	0.01	1.54	0.43	0.047
2H-2, 115–120	Rh	5.98	14.6	1.04	0.10	0.10	0.01	1.54	0.37	0.045
3H-1, 135–140	Rh	7.98	14.5	0.84	0.09	0.09	0.01	1.54	0.24	0.043
3H-2, 115–120	Rh	9.28	13.3	0.94	0.10	0.10	0.01	1.54	0.29	0.042
4H-1, 135–140	Rh	11.28	—	—	—	—	—	—	—	—
4H-2, 92–97	Rh	12.35	12.5	0.79	0.09	0.09	0.01	1.56	0.29	0.030
347-M0064D-										
1H-1, 130–135	Rh	1.35	12.8	0.92	0.10	0.10	0.02	1.55	0.89	0.044
1H-2, 92–97	Rh	2.47	13.3	0.87	0.09	0.09	0.02	1.54	0.74	0.046
2H-1, 130–135	Rh	3.55	13.9	0.87	0.08	0.08	0.01	1.55	0.59	0.045
2H-2, 110–115	Rh	4.85	14.2	0.81	0.08	0.08	0.01	1.54	0.41	0.044
3H-1, 130–135	Rh	6.85	14.3	0.82	0.08	0.08	0.01	1.55	0.28	0.040
3H-2, 111–116	Rh	8.16	14.6	0.97	0.09	0.09	0.01	1.55	0.28	0.038
4H-1, 130–135	Rh	10.15	13.5	0.89	0.09	0.09	0.01	1.55	0.31	0.027
4H-2, 110–115	Rh	11.45	12.0	0.75	0.08	0.08	0.01	1.57	0.27	0.022
5H-1, 130–135	Rh	13.45	—	—	—	—	—	—	—	—
5H-2, 110–115	Rh	14.75	12.5	0.88	0.10	0.10	0.01	1.57	0.37	0.023

Rh = Rhizon sample. — = no data are reported for samples with insufficient pore water volumes.

Table T5. Total carbon (TC), total organic carbon (TOC), total inorganic carbon (TIC), and total sulfur (TS) in sediment, Site M0064.

Core, section, interval (cm)	Depth (mbsf)	TC (wt%)	TOC (wt%)	TIC (wt%)	TS (wt%)
347-M0064A-					
1H-1, 13–14	0.13	2.66	2.29	0.36	0.81
1H-1, 51–52	0.51	0.43	0.20	0.23	1.06
1H-1, 90–91	0.90	0.72	0.29	0.43	0.13
2H-1, 110–111.5	4.10	1.33	0.47	0.87	0.16
3H-1, 64–65	6.94	1.31	0.54	0.77	0.20
3H-1, 83.5–84.5	7.14	3.45	1.75	1.69	0.39
3H-1, 110–111	7.40	1.75	0.46	1.29	0.20
7H-1, 32–33	16.37	3.09	0.19	2.90	0.36
10H-1, 17–18	18.67	1.93	0.28	1.65	0.40
12H-1, 4–5	20.54	1.87	0.37	1.51	0.52
15H-1, 28–29	23.78	2.01	0.34	1.67	0.43
18H-1, 62–63	27.12	1.85	0.29	1.57	0.37
20H-1, 26–27.5	28.76	1.61	0.28	1.33	0.44
22H-1, 68–69	31.18	1.93	0.27	1.66	0.47
24H-1, 21–22	33.71	2.16	0.31	1.85	0.41
26H-1, 70–71	36.20	2.25	0.26	1.99	0.30
28H-1, 5–6	37.55	2.16	0.28	1.88	0.31
347-M0064B-					
1H-1, 80–81	0.80	1.52	0.61	0.91	0.14
1H-3, 30–31	3.00	1.53	0.45	1.09	0.14
2H-1, 75–76	4.05	3.19	0.32	2.86	0.38
2H-2, 81–82	5.61	1.33	0.10	1.23	0.18
3H-2, 19–20	7.11	1.85	0.09	1.76	0.21
347-M0064C-					
1H-1, 87–88	0.87	1.92	0.47	1.44	0.17
1H-3, 26–27	3.05	1.55	0.47	1.08	0.14
2H-1, 60–61	3.90	1.76	0.55	1.21	0.16
2H-3, 4–5	6.14	1.65	0.48	1.17	0.15
3H-1, 30–31	6.90	1.74	0.45	1.29	0.16
3H-1, 80–81	7.40	1.86	0.14	1.72	0.23
3H-2, 20–21	8.30	3.44	0.26	3.18	0.37
4H-1, 37–38	10.27	2.67	0.26	2.41	0.36
5H-1, 23–24	12.93	3.19	0.25	2.94	0.33
6H-1, 56–57	14.26	2.33	0.23	2.09	0.28
13H-1, 78–79	22.48	3.06	0.24	2.81	0.35
15H-1, 85–86	24.55	3.45	0.30	3.14	0.37
16H-1, 57–58	25.27	2.06	0.27	1.78	0.45
18H-1, 72–74	27.42	2.07	0.28	1.79	0.37
20H-1, 65–66	29.35	1.98	0.29	1.68	0.47
21H-1, 37–39	30.07	1.94	0.29	1.66	0.87
22H-1, 57–58	31.27	1.90	0.26	1.64	0.40
24H-1, 100–101	33.70	2.26	0.27	1.99	0.39
26H-1, 82–84	35.52	1.93	0.26	1.67	0.30
28H-1, 71–73	37.41	2.05	0.27	1.78	0.34
347-M0064D-					
1H-1, 65–66	0.65	2.87	2.38	0.49	1.44
1H-2, 65–66	2.15	0.30	0.23	0.06	0.11
2H-1, 90–91	3.10	1.79	0.48	1.31	0.16
3H-1, 130–131	6.80	1.36	0.47	0.89	0.24
3H-2, 100–101	8.00	1.53	0.49	1.03	—
4H-1, 49–50	9.29	2.37	0.38	1.99	—
4H-2, 84–85	11.14	3.09	0.23	2.86	0.38
5H-1, 35–36	12.45	3.09	0.26	2.83	0.40
5H-2, 49–50	14.09	3.59	0.23	3.36	0.42
7H-1, 53–54	16.93	2.73	0.23	2.50	0.24
8H-1, 66–67	18.06	2.82	0.11	2.70	0.31
8H-1, 57–58	17.97	1.87	0.24	1.63	0.22
15H-1, 40–41	25.80	2.58	0.23	2.35	0.38
16H-1, 20–21	26.60	1.89	0.27	1.62	0.42
18H-1, 70–71	29.10	2.15	0.25	1.90	0.36
19H-1, 23–24	29.63	1.85	0.25	1.60	0.38
21H-1, 37–38	31.77	2.30	0.25	2.05	0.40
22H-1, 21–22	32.61	1.61	0.26	1.34	0.34
23H-1, 7–8	33.47	2.29	0.27	2.02	0.39

Table T6. Composite depth scale, Site M0064.

Core	Offset (m)	Top depth (mbsf)	Top depth (mcd)
347-M0064A-			
1H	0.44	0.0	0.44
2H	0.14	3.0	3.14
3H	0.63	6.3	6.93
4H	0.63	9.6	10.23
5N	0.63	12.9	13.53
6P	0.63	15.9	16.53
7N	0.63	16.1	16.68
8N	0.63	16.5	17.13
9N	0.63	17.5	18.13
10N	0.63	18.5	19.13
11N	0.63	19.5	20.13
12N	0.63	20.5	21.13
13N	0.63	21.5	22.13
14N	0.63	22.5	23.13
15N	0.63	23.5	24.13
16N	0.63	24.5	25.13
17N	0.63	25.5	26.13
18N	0.63	26.5	27.13
19N	0.63	27.5	28.13
20N	0.63	28.5	29.13
21N	0.63	29.5	30.13
22N	0.63	30.5	31.13
23N	0.63	31.5	32.13
24N	0.63	33.5	34.13
25P	0.63	34.5	35.13
26N	0.63	35.5	36.13
27N	0.63	36.5	37.13
28N	0.63	37.5	38.13
29N	0.63	38.5	39.13
30N	0.63	39.5	40.13
31S	0.63	40.5	41.13
32N	0.63	40.5	41.13
347-M0064B-			
1H	4.91	0.0	4.91
2H	4.91	3.3	8.21
3H	4.91	6.6	11.51
347-M0064C-			
1H	1.73	0.0	1.73
2H	1.73	3.3	5.03
3H	1.73	6.6	8.33
4H	1.73	9.9	11.63
5N	1.73	12.7	14.43
6N	1.73	13.7	15.43
7N	1.73	14.7	16.43
11N	1.73	19.7	21.43
12N	1.73	20.7	22.43
13N	1.73	21.7	23.43
14N	1.73	22.7	24.43
15N	1.73	23.7	25.43
16N	1.73	24.7	26.43
17N	1.73	25.7	27.43
18N	1.73	26.7	28.43
19N	1.73	27.7	29.43
20N	1.73	28.7	30.43
21N	1.73	29.7	31.43
22N	1.73	30.7	32.43
23N	1.73	31.7	33.43
24N	1.73	32.7	34.43
25N	1.73	33.7	35.43
26N	1.73	34.7	36.43
27N	1.73	35.7	37.43
28N	1.73	36.7	38.43
29N	1.73	37.7	39.43
347-M0064D-			
1H	–0.40	0.0	–0.40
2H	–0.31	2.2	1.89
3H	–0.08	5.5	5.42
4H	–0.08	8.6	8.52
5H	–0.08	12.1	12.02
7N	–0.08	16.4	16.32
8N	–0.08	17.4	17.32
11N	–0.08	20.4	20.32
12N	–0.08	21.4	21.32
15N	–0.08	25.4	25.32
16N	–0.08	26.4	26.32
18N	–0.08	28.4	28.32
19N	–0.08	29.4	29.32
21N	–0.08	31.4	31.32
22N	–0.08	32.4	32.32
23O	–0.08	33.4	33.32

Table T7. Splice tie points, Site M0064.

Hole, core, section, interval (cm)	Depth (mbsf)	Depth (mcd)		Hole, core, section, interval (cm)
347-				347-
M0064D-1H-2, 73	1.39	1.83	Tie to	M0064A-1H-1, 139
M0064A-1H-3, 19	3.65	3.34	Tie to	M0064D-2H-1, 144
M0064D-2H-2, 134	4.59	4.73	Tie to	M0064A-2H-1, 159
M0064A-2H-3, 49	4.60	6.33	Tie to	M0064C-2H-1, 130
M0064C-2H-3, 42	7.62	8.25	Tie to	M0064A-3H-1, 131
M0064A-3H-2, 91	7.62	9.35	Tie to	M0064C-3H-1, 101
M0064C-3H-3, 41	9.81	11.54	Append	

Table T8. Sound velocities, Site M0064.

Unit	TWT (ms)	Thickness of unit (m)	Sound velocity (m/s)*	Depth (m)	Depth (mbsf)
Seafloor	0.0811	59.8	1475	59.80	0.00
I	0.0829	1.34	1450	61.14	1.34
II	0.0835	0.41	1500	61.55	1.75
IIIa	0.0919	6.12	1449	67.67	7.87
IIIb	0.0938	1.43	1530	69.10	9.30
IVa	0.1116	16.1	1807	85.20	25.40
IVb	0.1241	11.3	1804	96.50	36.70
IVc	0.1332	8.3	1825	104.80	45.00

* = sound velocities are based on values measured during the OSP.